PIXEL-BASED AND OBJECT-BASED CLASSIFICATION METHODS FOR SURVEYING WETLAND VEGETATION WITH AN UNMANNED AERIAL SYSTEM

by

Nicholas R Villarreal, B.S.

A thesis presented to the Graduate Council of
Texas State University in partial fulfillment
of the requirements for the degree of
Masters of Science
with a Major in Geography
August 2016

Committee Members:

Jennifer L.R. Jensen

Thomas B. Hardy

Nathan Currit

FAIR USE AND AUTHOR’S PERMISSION STATEMENT

Fair Use

Duplication Permission

DEDICATION

For Mrs. Shirley Fay Sample,

Let this be a small token of appreciation for being the bold woman you are. This is entirely your fault and a direct consequence of the sacrifices you made to pursue your education. You left Green Bay for New Mexico with the world against you, just a silly young woman with no place in university. Fearless, open-minded individuals like yourself led the way for generations of women and minorities who have a place in higher education today. Thank you for sharing the natural beauty of this incredible place we call home.

ACKNOWLEDGEMENTS

First, I would like to thank my advisor and committee chair Dr. Jennifer L.R. Jensen, whose clever and logical insight of an intricate and rapidly evolving field, is truly a humbling and a complete privilege to witness. Completion of this thesis would not have been feasible, if not for her endless encouragement, eloquence in sarcasm, and intelligent outlook. Furthermore, her dedication to propel this department's research capabilities into uncharted territory, and challenge young geographers to be well-seasoned scientists, has been more than an inspiration, and altered the trajectory of my future. In the matter of a couple of semesters, I went from an undergraduate who was eager to finish his education, to a motivated senior applying to the graduate program, because he actually believed he just might have a chance of being accepted.

I would also like to thank, Drs. Thomas B. Hardy and Nathan Currit. Dr. Hardy's patience and generosity provided the opportunity to discover innovative research interests, to explore unimaginable places, to contribute to a talented team of incredible academics, to absorb priceless hands-on experience with prominent remote sensing veterans, and to tackle the distinctive assignment that became my focus as a graduate student. His commitment to pioneering innovative research systems, has established an unparalleled footing for what will become my passion and future expertise. Dr. Currit's exceptional evaluation and valued recommendations were essential to reinforce the utility and consistency of this research. Without his thoughtful critique and committed proficiency to the foundations of remote sensing, this thesis would be lacking the transparency and necessary considerations to thorough completion of this research.

In addition, I would like to thank my parents, Mario and Betsy Villarreal, and Jacob Villarreal, my best friend and brother. They have always believed in my pursuit of happiness, even when it initially concerned them, and required patience for a backseat driver still stuck in his car seat, who occasionally told the sun to go away with great frustration. Without their trust and the sacrifices they made, this would not have materialized. Furthermore, I would like to thank all the loved ones from the Garcia, Rico, Sample, and Villarreal families, for the essential advice they provided and the perpetual source of support and inspiration they were throughout this process.

I would like to thank my grandparents, William and Shirley Sample, their leadership, complete support, and commitment to encouraging awareness of the natural world, along with it's past, enthused an illiterate young explorer, equipped with a map of my own to decipher. I have to thank my grandparents, Romeo and Paulina Villarreal, we have never met, yet the strength of your character, and the depth of the loving support you shared with our family is treasured more with each passing day. I have heard recollections of the advice Popo shared with his children as long as I can remember, "Whatever you do, make sure you get your education, because they can never take that away from you." My Tia mentioned if only he knew his grandson went to school to mess around with drones, he would laugh, "mijo, that's not what I meant when I said get your education."

TABLE OF CONTENTS

LIST OF TABLES

LIST OF FIGURES

Figure **Page**

LIST OF ABBREVIATIONS

Abbreviation	**Description**
LAI	Leaf Area Index
MMU	Minimum Mapping Unit
NDVI	Normalized Vegetation Difference Index
NIR	Near-infrared
OBIA	Object-based Image Analysis
PBSIA	Pixel-based Spectral Image Analysis
RGB	Red Green Blue
RCWMA	Richland Creek Wildlife Management Area
UAS	Unmanned Aircraft System

1.0 INTRODUCTION

1.1 Background

Wetlands are areas of land covered with shallow water or have soil saturated with moisture (Merriam-Webster). Descriptions of wetlands can vary widely as there are several different types of wetlands across the globe, including bog, bottomland, fen, marsh, mire, moor, muskeg, peatland, prairie potholes, riparian, slough, swamp, wash, and wet meadow. The criteria for what constitutes a wetland has been extensively debated in the U.S. Supreme Court throughout several cases because determining where wetlands begin and end has proven difficult (*SWANCC V.USACE*, *Carabell V. USACE.).*The ruling in *Rampanos V. U.S.* has left wetland designation cases to be decided on a case-by-case basis because adequately defining the complex variations between all of the nation's wetlands is impossible (*Rapanos V. U.S.*).

Wetlands have been the focus in U.S. Supreme Court cases because they maintain critical ecological processes that enhance water quality, support diverse habitats, and include some of the most abundant and economically valuable ecosystems in the world as they produce vital ecosystem services from the peatlands of the Andes to the mangroves of West Africa. Only half of the wetland ecosystems existing in the early 20th century remain today in Australia, China, Europe, and North America (Moreno-Mateos et al. 2012). The growing effects of climate change threaten to accelerate wetland loss and sustainable management will be essential to preserve the benefits provided by productive wetland ecosystems (Tiner et al. 2015).

Historically, wetlands have been considered wastelands, a useless landscape that ought to be filled in, destroyed, stripped of lumber and forgotten. Only recently has society recognized the environmental services and necessity of natural wetlands. Wetlands can act as “nature’s wastewater treatment facility”, coastal wetlands can serve as critical storm buffers, marshes collect and contain seasonal flood waters, and prairie potholes provide vital nesting and migratory support for birds. The impacts of wetland loss can go unrecognized for several decades until the long term-consequences become noticeable, irreversible, and in some cases a direct threat to communities. For example, the vital and irreplaceable role of wetlands was obvious after rapid deterioration of Louisiana’s wetlands left coastal communities vulnerable to the harm of Hurricane Katrina and then Hurricane Rita (Houck 2015).

In the U.S., more than 50 percent of wetland area has been lost since the arrival of European settlers (Houck 2015). Wetland ecosystems are vulnerable to indirect damage from agricultural runoff, road building, and urbanization as these factors can result in hydrologic alterations that affect water supply, drainage patterns, and the size of ecosystems dependent on these water sources. Although the rate of wetland area loss has declined as wetland conditions have been restored on tens of thousands of hectares of land throughout the US (Whigham 1999; Faibairn and Dinsmore 2001), they are still a fragile ecosystem that requires monitoring (Tiner et al. 2015).

To mitigate the negative effects of wetland loss, land managers have tried to restore wetlands to recreate beneficial environmental processes. Constructed and restored wetlands attempt to mitigate the loss of natural wetlands, improve water quality, meet water supply demands, and support wildlife habitat. However, these efforts have resulted in varied degrees of success, and most have yielded ecological productivity levels significantly inferior than pre-degradation counterparts (Moreno-Mateos et al. 2012).

Wetlands are monitored with various assessment techniques and evaluated by several potential indicators that estimate the status of ecological health and productivity. At the landscape scale, GIS can be used to display wetland conditions for visual inspection and discriminate between wetland cover types. Wetland conditions can be modeled using large-scale land cover parameters such as continuity or fragmentation, perimeter buffer width and composition, density and proximity of roads, density of residential development, etc. Landscape level metrics are often used during the initial stages of wetland mapping to create a baseline dataset and potentially detect changes in wetland health. Routinely assessing spatial change of wetlands is necessary for effective implementation of comprehensive monitoring systems and more advanced methods of determining wetland productivity (Tiner et al. 2015).

Extensive field data collection can be employed to further evaluate wetland health by monitoring the wetlands and its established boundaries to estimate percent cover of invasive vegetation, a measure used to identify the physical, chemical, and biological stressors in and surrounding the wetland landscape. Determining wetland health and productivity with more accurate and detailed metrics requires resource intensive monitoring efforts that include comprehensive sampling needed to conduct an accurate biological assessment or index of biological integrity (IBI), and acquisition of relevant physical and chemical measurements. When feasible, extensive site level assessments of wetland conditions can provide a vital tool for managers or planners to effectively improve wetland protection measures (Tiner et al. 2015).

Measurements characterizing vegetation are most commonly used in evaluations of wetland restoration projects (Moreno-Mateos et al. 2012). Wetland vegetation is a prime indicator of ecosystem health and productivity, signaling the first signs of physical or chemical degradation (Adam et a. 2009). Mapping wetland vegetation type by distribution, quality, and quantity are most commonly used as assessment metrics (Adam et al. 2009). Having up-to-date spatial data about the status and condition of vegetation cover is essential to effectively conserve, maintain, or restore wetland vegetation.

Traditional wetland mapping practices are characterized by conducting excessive fieldwork with limited techniques, including visual estimation of percentage cover for each species, and often produce data with poor precision and questionable accuracy. Traditional field surveys are labor-intensive, costly, and require lengthy periods of time to complete. In some cases fieldwork isn't even feasible because of poor accessibility. The complications associated with wetland fieldwork limits practical application to relatively small areas (Adam et al. 2009).

Remote sensing datasets and GIS analysis have been applied to the monitoring of wetlands as early as the late 1990s and since then the number of studies investigating wetland species has increased as the capabilities of technology have grown. However, most remote sensing applications of wetlands are conducted with moderate or low spatial resolution imagery where the data are classified by general land cover; not by species (Table 1) (Whitehead et al. 2014). Traditionally, remote sensing datasets for wetland monitoring have relied on aerial photography and more recently satellite imagery, both often lacking not only spatial resolution but also temporal resolution as datasets must be processed and published before publicly available (Jensen et al. 2011).

Table 1. Image spatial resolution

Image Spatial Resolution	
low	larger than 30m
moderate	2 - 30m
high resolution	under 2m

Satellite imagery has the advantage of large-scale area acquisition when surveying and mapping on regional or global scales. Aerial photography can be much more expensive to collect as costs include employment of a pilot, a plane, and a remote sensing platform. However, aerial photography can be captured and processed quickly with higher spatial resolution than commercially available satellite imagery, potentially producing useful information for wetland resource managers (Sghair and Goma 2013). Sghair and Goma (2013) used remote sensing and GIS with ground truth data to test accuracy of classifying wetland vegetation change over large areas in the UK with Landsat Thematic Mapper (TM) data and aerial photography. Their study concluded that both forms of remote sensing data could provide valuable information for management of wetlands. Not surprisingly, results indicated that the traditional aerial photography yielded higher accuracy than the satellite imagery because it was of higher spatial resolution, and some vegetation classes inhabited areas that were smaller than the pixel size of the satellite imagery (Sghair and Goma 2013).

Most cost-affordable remote sensing datasets often maintain insufficient spatial and temporal resolution for efficient use by wetland managers. However, Unmanned Aircraft System (UAS) platforms offer an economical approach to capturing valuable data with high temporal resolution and in some cases, can permit simultaneous collection of ground truth data (Lechner et al. 2012). Acquiring imagery and mapping invasive wetland vegetation species in a timely manner allows wetland managers to quickly make assessments and promptly take effective measures (Zaman et al. 2011).

An emerging application of vegetation monitoring has been focused on using high spatial resolution imagery acquired from a UAS platform to perform species-level classifications (Moffet et al. 2013) However, traditional classification methods present specific challenges. The traditional method of image classification is pixel-based spectral imagery analysis (PBSIA) and operates by classifying each pixel independently based on their individual spectral values (Matinfar et al. 2007). PBSIA has been widely utilized for the classification of satellite imagery with low to moderate resolution. However, in some studies PBSIA classification of high-resolution imagery has resulted in questionable performance and unreliable accuracy, specifically if the area of interest is a heterogeneous landscape such as wetlands (Leachner et al. 2012). This is due to the fact that at high-resolution each pixel represents a much smaller area than at lower resolutions and can produce a high contrast of spectral characteristics within the same land cover class (Addink et al. 2007).

Utilizing object-based image analysis (OBIA) can potentially minimize the likelihood of the “salt and pepper” effect, a common disadvantage of PBSIA classification for heterogeneous landscapes (Benz et al. 2004, Dronova et al. 2012). The fundamental difference in these classification methods is that instead of classifying each pixel independently, OBIA classification operates by segmenting the imagery and grouping pixels into defined objects (Walter 2000). While PBSIA classifies the entire scene with the same algorithm, a variety of procedures may be used to apply contextual information and process different classified objects (Benz et al 2004). The primary advantage of OBIA includes the ability to increase spectral separation within an image and as a result may enhance the detection of individual wetland species (Walter 2000).

1.2 Problem Statement

In rural East Texas, the Richland Creek Wildlife Management Area (RCWMA) maintains a large-scale constructed wetland that occupies nearly 900 ha of wetland cover divided into 20 inundated cells or paddocks. RCWMA's first system of four wetland cells was operational in two years and all cells were operational a decade layer. RCWMA supports an abundance of wildlife and improves Trinity River water quality through bio-filtration to assist Tarrant Regional Water District's (TRWD) in meeting the water supply demands of the Dallas-Fort Worth Area. Trinity River water is cycled through a series of wetland cells over 6.5 days in order to reduce phosphorus, nitrogen, heavy metals, and other nutrients.

Current efforts to monitor vegetation type and abundance in the RCWMA involve time-consuming field surveys. Moreover, a complete map of vegetation composition is currently unavailable. This study will employ UAS-based remote sensing to classify vegetation within the RCWMA to establish baseline maps for which future imagery can be compared and thus, provide a relatively low-cost monitoring framework. Additionally, this study will assist in defining the accuracy and advantages/disadvantages of using pixel-based or object-based classification methods to survey wetland vegetation cover. Results will additionally assist in monitoring vegetation response to different management strategies, establishing annual growth rates, and evaluating habitat suitability for populations of indigenous and migratory bird species.

1.3 Research Objectives

This research will address the following objectives:

> Objective 1: Perform PBSIA and OBIA classification on UAS imagery acquired in 2014
>
> Objective 2: Compare accuracies resulting from the two classification methods used on UAS imagery acquired in 2014
>
> Objective 3: Use the more accurate classification method identified in objective 2 to classify UAS imagery acquired in 2015 and perform post classification change detection

1.4 Justification

The completion of this research is necessary because it is of interest to natural and constructed wetland managers who seek to survey and monitor their wetlands. Research regarding the mapping of constructed wetlands is limited as the science of wetland restoration is an emerging field. Constructed wetlands and wetland landscapes in general are commonly mapped at low to moderate resolution. Moreover, when higher-resolution imagery is used, most studies lack species-level classification and are more commonly classified by general land cover type. This research provides a unique case study in mapping constructed wetland vegetation at the species level with high-resolution UAS imagery and a comparative analysis of the accuracies between two remote sensing classification methods.

Benefits of this research include a documented analysis of two well-known methods, detailing reasons for differences in accuracy, and the practical advantages/disadvantages for both. The findings detailed within this study can assist natural resource managers in determining which method is more applicable to meet individual specific goals based on their area of interest, desired accuracy, temporal and spatial resolution availability, species class priority, and availability of financial or technological resources.

2.0 LITERATURE REVIEW

2.1 Ecological role of wetlands and wetland construction/restoration

Wetlands provide habitat for an array of amphibians, invertebrates, and populations of indigenous and migratory bird species. These habitats are vital as their heterogeneous hydrology and soil composition enable a robust mix of ecological niches that maintain high biodiversity (Sghair and Goma 2013).

Research has confirmed that wetland bird species can populate a restored wetland in just a few years but certain species of birds are initially less likely to be found in restored wetlands until vegetative communities are more developed (Fairbairn and Dinsmore 2001). Eventually the vegetative and bird communities of restored wetlands become more similar to those of natural wetlands (Young 1999).

"Because vegetation plays a critical role in nutrient cycles and productivity of many terrestrial and aquatic systems, accurate classifications of plant cover from remote sensing data are essential for broad-scale assessments of ecosystem structure and dynamics," (Dronova et al.2012). North American resource agencies invested 70 billion dollars in an attempt to restore 3,000,000 ha of wetlands (Moreno-Mateos et al. 2012).Awareness of their environmental and functional value has increased in recent years. Wetlands maintain several environmental processes including flood mitigation, groundwater recharge, carbon sequestration, erosion regulation, and water filtration (Sghair and Goma 2013). From 1991 to 2011, *2.2 Constructed wetlands management and monitoring*

Constructed wetlands are treatment systems that recreate the natural functions of wetland vegetation, soils, and their microbial accumulation for the primary purpose of enhancing water quality (EPA 2004). Constructed wetlands offer unique scientific research opportunities as their long-term dynamics are not well studied The science of wetland restoration and creation is still in its early stages with limited information available to ensure wetlands are constructed with a high degree of success. Understanding the distribution of wetland vegetation is essential to assessing the health of wetland ecosystems and accurate mapping of wetland vegetation has been a goal of science, environmental management, and restoration (Moffet et al. 2013).

Multifunctional wetlands provide a range of benefits including flood prevention, wildlife food and habitat production, aesthetic beauty, and educational and recreational uses. Constructed wetlands are also low-carbon systems that require minimal engineering infrastructure and simple management practices, making them an ideal alternative to wastewater treatment facilities (Semeraro et al. 2015, Masi et al. 2013).
Over the past decade, constructed wetlands have become more common in developed countries. Constructed wetlands treatment is not a new concept as over 5,000 constructed wetlands have been built in Europe and approximately 1,000 are currently operating in the U.S. (EPA 2004).

Constructed wetlands must be designed with careful consideration of site-specific conditions, including vegetation, hydrology, soil suitability, and presence of endangered species. If the wetland location has highly permeable soil an impervious clay liner can be used and original soil is applied on top. Depending on local factors wetland vegetation can be planted or left to develop naturally. Adequate water control structures must be installed to provide efficient response to any alteration in water quality, depth, and flow. Constructed wetlands are typically built on highlands located in the flood plain as a precaution to limit impairment of any proximate aquatic resources in the event of a minor flood. Most constructed wetlands are formed through iterations of excavating, backfilling, and grading, followed by installation of water control infrastructure. Appropriate precautions must be taken during each phase of wetland construction to prevent harmful environmental repercussions, such as disruption of natural hydrology, or the onset of an invasive plant species.

In Southern Italy a small-scale artificial wetland system has been successfully utilized to provide multiple benefits and mitigate the effects of 60 years of urban sprawl. The 8.3 ha facility was constructed and operational within only a year. With only 5.1 ha of actual wetland cover the operation treats the wastewater of approximately 41,000 inhabitants from three municipalities and still manages to preserve the aesthetic value critical to tourism in the area (Semeraro et al. 2015, Masi et al. 2013).

Mapping and monitoring of wetland vegetation is a goal of science, management, and restoration because patterns can serve as great indicators of wetland health and development. The demand for wetland mapping continues to grow as the global population increases and the importance of wetlands becomes more widely recognized as their complex dynamics are better understood (Tiner et al. 2015). Management of wetlands typically entails monitoring development of vegetation over a certain period of time. Valid identification of invasive species is an integral component of wetland management as it assists in application of adequate control practices. Traditionally, wetland vegetation estimates involved conducting transect field surveys, which required more labor, time, and the disturbance of fragile ecosystems. Today, remote sensing technologies provide a more efficient, less intrusive technique for surveying wetland vegetation (Moffet et al. 2013). Accounting for distribution patterns in wetland vegetation is an essential component to understanding the complex ecological and hydrologic processes (Moffet et al. 2013). The science of mapping wetlands for monitoring purposes has advanced over several decades; from transect surveying to interpreting aerial photographs, and more recently by employing advanced remote sensing data, including the tools associated with remote sensing technologies (Tiner et al. 2015).

2.3 Remote Sensing of Wetlands

Numerous researchers have applied both multispectral data including Landsat TM and SPOT imagery to classify general vegetation communities and hyperspectral data to define wetland vegetation at the species level. In addition, remote sensing methods have progressed to estimating biophysical and biochemical characteristics of wetland vegetation, such as leaf area index (LAI), biomass and water content.

While remote sensing capabilities have expanded, the data produced is only an image, and not the actual information desired (i.e., a detailed map of vegetation distribution). The image simply captures electromagnetic radiation from the surface and in wetlands this often results in very low contrast between landscape features (Moffet et al. 2013). Remote sensing vegetation indices are derived from absorption, transmittance, and reflectance of vegetation in the red and near infrared regions of the electromagnetic spectrum. Research has demonstrated that the ratio of near infrared and red correlate directly with levels of biomass (Lyon et al. 1998). Most vegetation indices take advantage of this effect by formulating basic algorithms, including subtraction of the near-infrared and red, division of near infrared by the red, and combining both to produce a normalized difference vegetation index (NDVI) (Lyon et al. 1998).

Another method of wetland mapping and monitoring with remote sensing data involves image classification and post-classification comparison methods. Baker et al. (2007) applied these techniques to determine the total area of change within a restored wetland. In restored wetlands, using landscape parameters at high spatial resolution for detecting pattern difference is difficult, and selection of a minimum mapping unit selection is crucial. While Baker et al. (2007) concluded that health of habitat is not limited to only measures of abundance, Kelly et al. (2011) added that configuration and heterogeneity are also important factors. Investigation of wetland vegetation changes in the UK indicated that different types of imagery created classification outcomes with a range of accuracies (Sghair and Goma 2013). With some exceptions, the majority of research conducted on remote sensing applications to wetlands has been limited to the moderate or low resolution of publicly available satellite imagery. In some cases, lack of resolution can limit classifications to broad scales and general land cover classes. Today, alternative platforms are becoming more affordable and highly detailed classification schemes will likely replace broad scale remote sensing trends (Whitehead et al. 2014).

The number of studies exploring the application of remote sensing to investigate wetland species has rapidly increased since the late 1990s, coinciding with advancements and commercialization of technology related to remote sensing platforms, including sensors and computer processing power.(Adam et al. 2010). These advancements are also responsible for the increased implementation of unmanned aircraft systems (UAS) for remote sensing applications (Lyon et al. 1998).

2.4 UAS remote sensing

Most remote sensing systems used to survey the distribution of vegetative species are either too expensive to utilize consistently or lack efficient temporal resolution to be of significant value to resource management (Jensen et al. 2011). High-resolution imagery used for vegetation classification is generally collected with a fixed-wing manned aircraft. However, this form of acquisition is often very expensive; and the UAS platform offers a similar product at lower cost. High spatial and temporal resolutions are requirements for producing useful remote sensing products that monitor vegetation in a timely manner so that findings may support resource managers on use of appropriate techniques (Whitehead et al. 2014).

UAS platforms often cost less money than traditional acquisition of very high-resolution satellite remote sensing data and UAS's can collect more accurate data (Jensen et al. 2011). At low flight altitudes, UAS's may operate with an inexpensive camera to collect imagery at meter to sub-meter spatial resolution and fine scale temporal resolution ranging from minutes to hours. However, low altitude data acquisition also decreases the footprint size or the total area that each image can cover. Smaller footprint size requires more processing and georeferencing work in order to accurately stich images together (Jensen et al. 2011).

This limitation may create two significant disadvantages for UAS remote sensing referred to as the coverage control problem and the georeference problem. The coverage control problem requires UAS technicians to closely check the UAS's flight path multiple times and ensure adequate coverage of the entire area (Jensen 2008). The georeference problem involves precise alignment of each pixel from the UAS images with the appropriate GPS coordinates during or after image acquisition. In addition to these main limitations, small footprint size can lead to challenging circumstances when surveying a large-scale site due to the time-consuming nature of UAS image acquisition and limited flight times (Jensen 2008).

There are two different solutions to the two major complications of UAS remote sensing called the open-loop and closed-loop solution. The open-loop solution addresses the problems independently, meaning that the coverage control problem is resolved prior to acquisition and the georeferencing problem resolved after image acquisition. The open-loop solution is straightforward and robust but dependent on a considerable degree of experience to appropriately calculate various settings including overlapping percentage and minimal camera shooting interval (Jensen 2008). Georeferencing complications can be resolved by performing feature-based stitching, a process that stitches images together using identifiable features as tie points. These features can manually be selected by the user or identified automatically with algorithms used by image processing software platforms. Automatic tie point identification is more effective if each photo shares at least a few common features, thus requiring the images to have sufficient overlap (Jensen 2008). The closed-loop solution addresses both problems simultaneously by utilizing georeferencing data in real-time, which allows the path planning controller to monitor each and every moment during flight. Another method uses positional data recorded by the UAS to map each individual image back to a relevant ground reference image and synchronizes each pixel with their corresponding ground coordinates (Jensen 2008).

UAS's can provide site-based image acquisition at high spatial resolutions, and the potential to collect imagery simultaneously with ground truth data (Lechner et al. 2012). Many of these platforms are feasible because of the recent miniaturization and commercialization of multispectral cameras (Lyon et al. 1998). Once imagery is acquired, it is stitched together into mosaics, georeferenced, and used to classify vegetation for restoration monitoring (Zaman et al. 2011).

The suitability of UAS-derived hyperspectral imagery has been demonstrated by accurately delineating the composition of salt marsh vegetation (Silvestri et al. 2013). Another UAS platform was successfully employed to assess the extent of a swamp area using an object-based analysis for the classification of a hyper-spectral resolution dataset comprised of several hundred independent spectral bands. However, the purpose of the study limited classification to a broad two-class scheme (Lechner et al. 2012). The capabilities of object-based methods and ultra-high resolution UAS imagery are increasing as levels of pest infestation can be detected on a branch level by designating specific object features (Lehman et al. 2015).

2.5 Object-based Image Analysis

Object-based image analysis (OBIA) has typically been applied to wetlands using moderate resolution imagery, however, at 30 x 30 m, the data's value are limited, particularly in the highly heterogeneous landscapes of wetlands. OBIA is inextricably linked to multi-scale analysis concepts (Blaschke 2010). The primary operation of OBIA is segmentation, the division of the image into spatially continuous and homogenous areas referred to as image objects or image candidates (Conchedda et al. 2008). The process distributes neighboring pixels in image candidates by integrating spectral and shape parameters throughout a pair-wise clustering operation. Segmentation examines standard spectral values, but also addresses region-oriented properties such as context, texture, structure, size, and shape. Each stage of the pair-wise clustering function merges couples of image candidates that create the least increase of variance. This iterative optimization procedure terminates when the least increase is greater than the parameter set. Parameters apply to primary object characteristics, such as texture, shape, color, and heterogeneity-defined weights. Segmentation applied at multiple scales with separate scale parameters permits the creation of hierarchical networks between objects. These networks construct relationships between objects at each scale, creating sub- and super-object interactions that can be used multiple times throughout the classification (Conchedda et al. 2008).

Advantages of using OBIA include a lower likelihood of producing outputs influenced by the salt-and-pepper effect prominent in PBSIA (Dronova et al 2013). The salt-and-pepper effect can be described as the distribution of speckled pixels between different classes (Benz et al 2004), for which PBSIA classifications are common. While the salt-and-pepper effect can be minimized for PBSIA classifications, this requires additional post-processing techniques such as applying a low-pass filter.

Since OBIA offers hundreds of variables, combinations, and overall options, this essentially allows endless revision and reclassification of OBIA classification outputs, as well as the application of expert knowledge-based interpretation. However, OBIA classification can require an extensive dedication of time as hundreds of variables and combinations can burden the investigator with an overwhelming plethora of information and decisions (Benz et al. 2004). For example, if compact circular assemblages of vegetation characterize the distribution of a particular wetland species typically found in clusters, this knowledge can be applied to the classification through utilization of relevant object feature statistics such as, elliptical nature, compactness, dissimilarity, and distance to sub-object neighbor of the same class (Lechner et al. 2012). General advantages of OBIA include relevant statistic and texture processing that enhance separation of classes within the feature space, including the use of numerous features such as length, shape, or number of edges, and incorporating relationships between super and sub-object neighbors (Benz et al. 2004). Ultimately, this increases the transparency between real-world objects and the image objects used to classify the imagery because OBIA is intrinsically linked to multi-scale analysis (Benz et al. 2004). High-resolution imagery provides a situation in which the specific advantages and flexible nature of OBIA can be fully utilized (Blaschke 2010).

High-resolution data using OBIA provides an alternative method to monitoring wetland cover. Typically, it is difficult to separate heterogeneous wetland features based on only spectral information of single pixels without the inclusion of surrounding spectral characteristics at a range of broad scales(Benz et al. 2004). Research has demonstrated that methods of segmentation and class hierarchy can be beneficial in swamp or wetland areas where vegetation species lack spectral contrast (Lechner et al. 2012).

Despite several potential benefits offered by OBIA, several problems can arise with this method. Segmentation, the first step required to perform an OBIA classification, can be a disadvantage if the image is difficult to segment in a manner that represents the reality of vegetation distribution, and requires several iterations of segmentation to produce an adequate output. If each class is not carefully considered during this crucial step, the segmentation level used may be insufficient, complications can arise during classification, and resulting maps may not meet accuracy requirements (Lechner et al. 2012).

In addition to the challenges posed by high-resolution imagery, OBIA does not have the efficiency and minimal user input of PBSIA as it requires user-defined parameters for segmentation and classification. Another disadvantage of OBIA is related to processing time due to the extensive data required to calculate statistics for each object and the hundreds of feature variables that may be selected in a variety of combinations (Benz et al. 2004). However, OBIA processes can increase classification accuracy, because the user can apply expert background knowledge of the area to enhance interpretation (Benz et al. 2004). For example, if a certain wetland species is typically found in clusters and distributed as dense elliptical assemblages of vegetation, this information can be applied to the classification for that specific class. Separation between that specific class and all other classes is enhanced through utilization of relevant object feature statistics such as elliptical nature, density, dissimilarity, and distance to sub-object neighbor of the same class (Lechner et al. 2012).

Dronova et al. (2012) conducted research that tested image-segmentation scale suitability for the classification of six families of plant functional types and determined none of segmentation techniques consistently offered advantages over the others. This study concluded that automated segmentation techniques are useful for vegetation detection with OBIA and advocated a thorough consideration of the spatial scale for image segmentation (Dronova et al. 2012). OBIA techniques of image segmentation and texture analysis have been applied to ultra-high resolution imagery to accurately distinguish six vegetation classes throughout riparian areas (Ehlers et al 2006).

2.6 Comparison of OBIA and Pixel-based Spectral Image Analysis

OBIA can improve classification accuracy of different plant species in complex wetland landscapes, compared to the traditional pixel-based spectral image analysis (PBSIA) (Matinfar et al. 2007). The main differences between methods are that in a traditional PBSIA classification, each pixel is classified independently, and in OBIA classification, all pixels within defined objects are included to define spectral behavior through an iterative classification process (Walter, 2000).

Desclée et al. (2006) tested the suitability of object-based techniques for detecting forest land cover change and results were compared to pixel-based outputs. The study crafted a new method to map land cover changes in forest by exploiting image segmentation, image differencing, and statistical analysis. Using high spatial resolution imagery, their method offers a straightforward approach that can be applied according to site-specific variables. The new technique was also assessed with multi-date SPOT-HRV imagery and accuracy was compared to the pixel-based method utilizing RGB-NDVI approach. The OBIA approach minimized the processing time because pixels were aggregated and reduced to segmented objects. The object-based change detection method outlined in the study resulted in accuracy higher than 90% and an overall Kappa coefficient of agreement greater than 0.80. This technique enhances change detection mapping because parameters and classification algorithms can be fine-tuned to the dynamics of each individual class and the site-specific conditions (Desclée et al. 2006).

Yu et al. (2006) applied an object-based approach to complete a comprehensive vegetation inventory at Point Reyes National Seashore in Northern California. Using high spatial resolution Digital Airborne Imaging System (DAIS) imagery, minimum image objects were produced with eCognition's Fractal Net Evolution Approach (FNEA). Fifty two spectral, texture, topographic, and geometric features were calculated for every object. A classification and regression tree algorithm (CART) was used to rank features by significance and apply the most valuable features to classification. The technique was tested against a pixel-based maximum likelihood classification (MLC) and effectively overcame the salt-and-pepper effect found in the pixel-based output by using minimum image objects. Significant increase in accuracy was accomplished by applying a hierarchical classification scheme and results well exceeded the 40 percent hurdle often encountered when remotely sensed data is used to map detailed vegetation classifications (Yu et al. 2006).

Matinfar et al. (2007) mapped land cover and land use in Iran with Landsat 7 Enhanced Thematic Mapper Plus (ETM+) data and compared pixel-based and object-based performance. An error matrix was produced using the same reference data and results indicated that OBIA was superior in overall accuracy for all land cover classes. Improved performance using the object-based method was a result of effective image segmentation and efficient handling of class hierarchy by the nearest neighbor classifier (Matinfar et al. 2007).

Finally, Conchedda et al. (2008) tested OBIA and PBSIA methods for mapping mangrove change in Southwestern Senegal. Using multispectral SPOT data, the OBIA approach included multi-resolution segmentation and definition of class-specific rulesets that integrated spectral values and patterns amongst objects at independent hierarchal levels. The study reported higher accuracy for PBSIA when mapping classes of change. The OBIA method mapped areas of mangrove decrease with poor accuracy and instead produced higher accuracy for mapping mangrove increase. OBIA accuracy was limited by the selected Minimum Mapping Unit (MMU) because any change smaller than the MMU was prevented from being detected. Advantages of OBIA included being straightforward and easy to replicate, class-specific ruleset development, application of user knowledge to improve change detection accuracy, and the ability to conduct change detection analysis without single-date classifications required (Conchedda et al. 2008).

Most of these comparative studies lack detailed species-group classification of wetland vegetation and utilization of ultra-high resolution imagery acquired by a UAS system. More importantly, few studies explicitly provide information on the feature properties applied or parameter values set in OBIA classification, and few justify how they determined these threshold values. Due to this fact, the majority of OBIA research is not straightforward and lacks detailed procedural information fit for precise replication.

3.0 MATERIALS AND METHODS

3.1 Study Area

Richland Creek Wildlife Management (RCWMA) is located in Fairfield, Texas, approximately 110 kilometers southeast of Dallas, Texas. The RCWMA encompasses 5,762 ha and includes a large constructed wetland (Figure 1). The wetland covers approximately 699 ha and incorporates an interconnected system of five sediment basins and twenty inundated cells. The area averages approximately 1 meter of annual rainfall, and is located downstream from the Richland-Chambers Reservoir, about half way in between Corsicana and Palestine, Texas. This places the site in an ecotone between the Post Oak Savannah and Blackland Prairie ecological regions.

RCWMA has identified several desirable vegetation species for wildlife habitat support. Desirable vegetation includes Algae (*Chlorophyta)*, Duckweed (*Lemna* L.), Sedge (*Abildgaardia* Vahl), Barnyard grass (*Echinochloa* P. Beauv.), Smartweed (*Polygonum* L), Burhead (*Echinodorus* Rich. ex Engelm), and a variety of Bulrush (*Schoenoplectus* (Rchb.) Palla)(USDA 2016). Smartweed and Barnyard grass are highly desirable as they provide ideal habitat for waterfowl and RCWMA is currently working to expand this habitat through innovative wetland management (USDA 2016). Identifying the most undesirable species of vegetation, Cattail (*Typha* L.), is of considerable importance for the RCWMA staff because it is capable of displacing the former desirable plant community (USDA 2016). Secondary nuisance plants include Sesbania (*Sesvania* Scop.) and American lotus (*Nelumbo lutea* Willd.). This process involves the movement of water through a wetland cell system comprised of two to four individual wetland cells.

Initially, nutrient-rich Trinity River water that is 95% effluent at low flow, releases into a primary cell and sits for a minimum of 6.5 days to guarantee adequate absorption of phosphorus, nitrogen, heavy metals, and other nutrients. The process repeats for all following cells and allows the former cells to dry out for several days. Next, the cells are prepared for the next flow by removing wetland bed soil containing the majority of unfavorable constituents. The last phase of this process involves the sediment basin where the final step of settling occurs at an ideal time of 8 hours. Wetland cell systems have been active for a range of time, from anywhere between six months to two years, and has subsequently resulted in distinctive cells that contain a variety of plant species, at different stages of development and abundance. Surveying wetland vegetation to estimate species distribution is essential to guaranteeing the success of this constructed wetland facility.

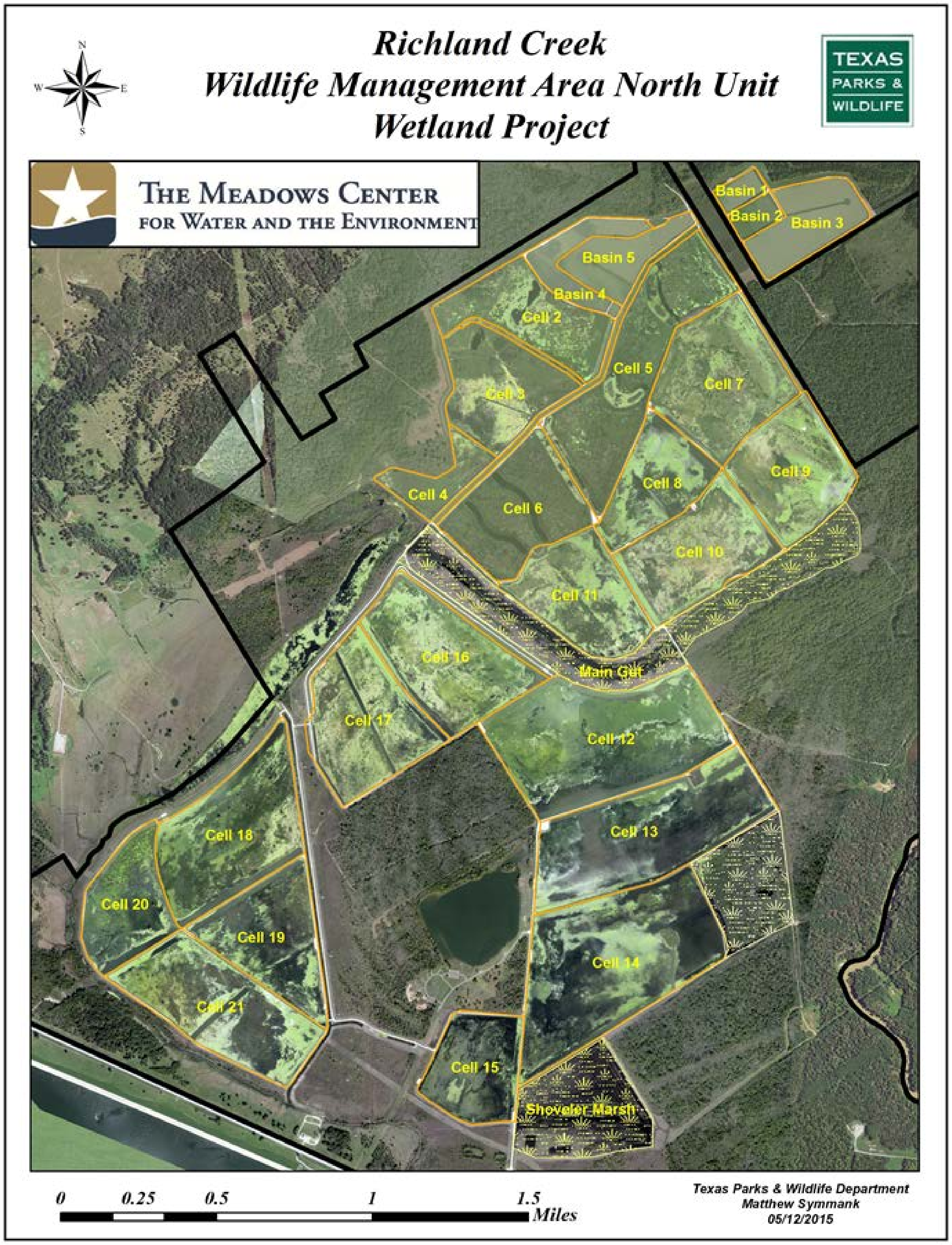

Figure 1. Study area

3.2 Image data acquisition

The Meadows Center for Water and the Environment (MCW) utilized an UAS system to conduct four flights and acquire 1,699 photos on October 31, 2014. The entire study area was broken into four overlapping flights to ensure adequate coverage of each of the 20 inundated cells. The images were acquired using two Canon digital cameras. The first camera acquired RGB imagery and measures spectral wavelengths between 400 -700 nm (Red, Green and Blue (RGB) wavelength intervals). The second camera acquired NIR imagery and measures spectral wavelengths between 700 – 1,200 nm (Near-Infared or NIR wavelength intervals). At the beginning of the flights imagery was captured at a minimum altitude of approximately 400 m and at a maximum altitude of 588 m. Most of the imagery was acquired at an altitude ranging between 571 m and 588 m. The four flights were conducted over a total time of 4 hours and 35 minutes, between the initial launch for flight 1 at 8:45am and the final retrieval of flight 4 at 1:20pm.

3.3 Image-processing

Pre-processing was conducted using Agisoft's Photoscan professional. Red-Green-Blue (RGB), and Near-infrared (NIR) mosaics for each flight were produced throughout a series of pre-processing steps. First, photos were aligned with recorded GPS data, followed by placement of marker coordinates to be used as ground control points. Then, camera alignment was optimized and followed by definition of the bounding box. The last steps included creating a dense point cloud, constructing a photo mesh, and finally generating an orthorectified photo.

After mosaics were finalized, NIR, red, green, and blue bands were exported independently for the calculation of the Normalized Difference Vegetation Index (NDVI) and final layer stacking. The final layer stacking creates one imagery file containing all five independent bands so that they can be utilized simultaneously for classification purposes. NDVI increases the spectral differentiation of vegetation and non-vegetation features by using an algorithm which divides the sum of the near-infrared band (NIR) and red band values, by the difference of the NIR and red band values (Zhan and Xie 2012). The final step in image processing is conducting a five-band layer stack consisting of red, green, blue, NIR and NDVI bands. Utilization of this five-band layer stack enables maximum spectral separation between five components of spectral values and optimal conditions to perform an accurate classification.

3.4 Vegetation data collection

Vegetation data were collected on October 5th, 6th, and 7th 2014. Samples were selected based on the guidance of Matthew Symmank's expert knowledge, and careful consideration of species importance, vegetation variability, density, and cell-specific characteristics. GPS data were collected by traveling cell-to-cell in field teams of 3 to 8 people. Trimble units were used to acquire GPS information and document species of vegetation as point and line features. After GPS features were processed they were ranked according to horizontal and vertical precision statistics. The most accurate and reliable features were selected for classification and confirmed by visual interpretation. Symmank's background information of the area was applied to digitize polygons of various species that lacked representation in certain wetland cells. All GIS data were segregated by class and each flight to increase ease of accessibility in ERDAS Imagine and eCognition Developer.

3.5 Image classification

Wetland vegetation cover was classified into eight management priority ranked classes: Class 1(Cattail), Class2 (Bullrush/Burhead/Toothcup), Class 3 (Spikerush/Sedge), Class 4 (Arrowhead), Class 5(Algae/Duckweed/Pondweed), Class 6 (Smartweed/Barnyard Grass/Millet), Class 7(Open Water/Submerged), and Class 8 (American Lotus/Primrose). For each class, the most accurate and precise GTD was selected, then compiled into datasets designated for each flight, and ultimately used to justify the assignment of classification to appropriate classes.

A supervised pixel-based classification was performed in ERDAS Imagine 2015. Spectral samples are collected using standard spectral distance values to ensure adequate coverage of vegetation assemblages, and are often class-specific. After class signatures have been adequately represented, classification is completed using a minimum distance to means classifier.

Next, eCognition Developer 64 8.4 (Trimble Germany GmbH 2015) was utilized to perform a supervised object-based classification by using image object feature statistics. These parameters include a priority class hierarchal structure correlated with the estimated class abundance and object-thresholds relative to each vegetation class. After inclusion of these object-specific parameters, objects for each class and respective spectral signatures are recalculated to include all pixels within class objects.

3.6 Accuracy assessment of classified images

Statistical analysis of classification accuracy was conducted using ERDAS Imagine. The accuracy assessment calculates the overall *kappa* and conditional *kappa* for each class, which represent agreement between classification results, and ground reference data, and an estimate of how much agreement is caused by chance. Other statistics produced by the assessment include producer's accuracy, user's accuracy, and overall accuracy. Producer's accuracy and user's accuracy are related to commission and omission error, respectively. Commission error refers to misclassification that occurs because pixels of another class are labeled by the user as belonging to the class of interest. Omission error takes place when pixels belong to the ground truth class, but are assigned to a different class (Conchedda et al. 2008). Error matrices for both classification methods were produced and compared. Resulting values for both the PBSIA and OBIA classification were then assessed to determine which vegetation classes were accurately classified.

3.7 Statistical analysis

The classifications for both methods and each flight were spatially joined using ESRI's ArcMap and a nearest neighbor algorithm. After the join was complete the area for both methods was calculated for all vegetation classes. Calculated area results for both classification methods were determined using the calculate geometry tool in ArcMap. The resulting spatial statistics assisted in further assessing the key differences between classification accuracy outcomes and understanding why vegetation area varies by class and by cell.

4.0 RESULTS

4.1 Results of 2014 PBSIA and OBIA classifications

The pixel-based method classified a total area of 354,167 m^2 for Class 1 (Cattail), 1,028,433 m^2 for Class 2 (Bulrush/Burhead/Toothcup) and 609,465 m^2 for Class 3 (Spikerush/Sedge),149,301 m^2 as Class 4 (Arrowhead), 2,783,367 m^2 as Class 5 (Algae/Pondweed/Duckweed), 448,351 m^2 as (Smartweed/Barnyard Grass/Millet), 131,422 m^2 as Class 7 (Open Water/Submerged), and 36,695 m^2 as Class 8 (American Lotus/Primrose) (Figure 2) (Table 2).

The object-based classification yielded a total area of 531,054 m^2 for Class 1 (Cattail), 656,226 m^2 for Class 2 (Bulrush/Burhead/Toothcup), 467,988 m^2 for Class 3 (Spikerush/Sedge), 252,375 m^2 for Class 4 (Arrowhead), and 2,885,467 m^2 for Class 5 (Algae/Duckweed/Pondweed) (Table 2). OBIA area totals classify 306,556 m^2 of Class 6 (Smartweed/Barnyard Grass/ Millet), 1,414,634 m^2 of Class 7 (Open Water/Submerged), and 269,459 m^2 of Class 8 (American Lotus/Primrose) (Figure 3) (Table 2).

In addition, class area totals for individual wetland cells were calculated in order to provide a comparison between the classification methods (Tables 3 and 4). The pixel-based classification resulted in minimum class area values in cell 15, including 66 m^2 for Class 1 (Cattail) and 254 m^2 for Class 2 (Bulrush/Burhead/Toothcup) (Table 3). Cell 12 represented maximum area values of 352,944 m^2 and 79,526 m^2 for Class 5 (Algae/Duckweed/Pondweed) and Class 6 (Smartweed/Barnyard Grass/Millet), respectively (Figure 2) (Table 3).

Object-based classification outcomes consist of minimum class values in cell 15, including 1,572 m^2 for Class 3 (Spikerush/Sedge), 1,525 for Class 6

(Smartweed/Barnyard Grass/Millet) and 154 m² for Class 1 Cattail, and 11 m² for Class 4 (Arrowhead) (Table 4). Maximum class values identified in cell 14 consist of 65,532 m² for Class 8 (American Lotus/Primrose), 157,473 m² for Class 2 (Bulrush/Burhead/Tootcup), and 217,976 m² for 7 (Open water/Submerged) (Figure 3) (Table 4).

The classifications share the most comparable maximum values in cell 5 for Class 1 (Cattail) as the difference between the OBIA and PBSIA area totals is 4,231 m². However, both methods produced contrasting results for most of the remaining classes and wetland cell area totals vary widely (Tables 3 and 4). Both classification results included maximum area values for Class 2 (Bulrush/Burhead/Toothcup) that were greater than any other class, excluding Class 5 (Algae/Duckweed/Pondweed) (Tables 3 and 4). Class 2 maximum area for the PBSIA classification totaled to 206,126 m², while the OBIA classification resulted in 157,473 m². The classification results also ended up with similar mean values for Class 5 (Algae/Duckweed/Pondweed) as the OBIA output averaged 144,273 m² and the PBSIA resulted in a mean of 133,168 m² (Tables 3 and 4). In addition, the classification outputs share nearly equal median values for Class 4 (Arrowhead) as the differed by only 36 m² (Tables 3 and 4). The object-based output yielded a median value of 5,347 m² and the pixel-based method resulted in a median value of 5,251 m² (Tables 3 and 4). While these area calculations provide similar values, the statistics associated with the results are mainly due to the different approaches employed by the classification method (Tables 3 and 4).

Table 2. Total area (m²) results for pixel-based and object-based classification of UAS imagery acquired in 2014

2014 - Total Area (m²) of Pixel-based & Object-based Classification Methods								
Class # Class Name / Method	**1 Cattail**	**2 Bulrush/ Burhead/ Toothcup**	**3 Spikerush/ Sedge**	**4 Arrowhead**	**5 Algae/ Duckweed/ Pondweed**	**6 Smartweed/ Barnyard Grass/ Millet**	**7 Open Water/ Submerged**	**8 Am. Lotus/ Primrose**
PBSIA	354,167	1,028,433	609,465	149,301	2,783,367	448,351	131,422	36,695
OBIA	531,054	656,226	467,988	252,375	2,885,467	306,556	1,414,634	269,459
Difference (OBIA - PBSIA)	176,887	-372,207	-141,477	103,074	102,100	-141,795	1,283,212	232,764

Table 3.Wetland cell class area (m²) results for pixel-based classification of UAS imagery acquired in 2014

2014 Pixel-based - Class Area by Wetland Cell (m²)								
Class	1 Cattail	2 Bulrush/ Burhead/ Toothcup	3 Spikerush/ Sedge	4 Arrowhead	5 Algae/ Duckweed/ Pondweed	6 Smartweed/ Barnyard Grass/ Millet	7 Open Water/ Submerged	8 Am. Lotus/ Primrose
Cell Number								
2	7,541	9,323	72,760	25,340	68,997	52,813	5,378	NA
3	16,465	33,675	78,141	9,149	68,096	25,925	15,939	NA
4	9,878	3,965	31,259	3,965	7,933	12,240	3,018	NA
5	122,455	53,329	118,144	5,251	74,932	52,467	8,398	NA
6	58,180	94,778	86,339	4,175	10,297	62,572	30,724	NA
7	9,733	25,997	20,918	25,997	286,806	22,286	4,559	NA
8	6,169	20,503	21,896	9,817	102,136	9,469	12,876	NA
9	2,319	1,984	12,476	9,293	245,798	26,447	1,988	NA
10	3,796	8,490	4,774	6,529	259,033	28,665	10,544	NA
11	11,106	3,668	8,152	307	212,857	2,727	37,998	NA
12	639	6,751	NA	NA	352,944	79,526	NA	NA
13	5,941	172,368	NA	NA	94,625	NA	NA	NA
14	NA	NA	NA	2,132	179,569	66,075	NA	36,695
15	66	254	NA	NA	129,144	NA	NA	NA
16	19,165	45,198	117,081	19,078	114,604	3,626	NA	NA
17	29,929	38,663	106,551	19,030	105,824	2,503	NA	NA
18	2,881	206,126	327	1,249	157,750	NA	NA	NA
19	4,654	55,848	6,197	3,139	64,509	879	NA	NA
20	12,413	54,340	5,183	4,043	54,340	NA	NA	NA
21	24,250	193,173	2,255	807	193,173	131	NA	NA

Table 4. Wetland cell class area (m²) results for object-based classification of UAS imagery acquired in 2014

2014 Object-based - Class Area by Wetland Cell (m²)								
Class	1 Cattail	2 Bulrush/ Burhead/ Toothcup	3 Spikerush/ Sedge	4 Arrowhead	5 Algae/ Duckweed/ Pondweed	6 Smartweed/ Barnyard Grass/ Millet	7 Open Water/ Submerged	8 Am. Lotus/ Primrose
Cell Number								
2	66,101	22,649	19,517	23,838	66,102	29,317	11,603	NA
3	76,585	23,210	22,297	22,117	64,690	17,904	19,207	NA
4	34,995	6,458	9,008	6,156	19,371	8,829	3,560	NA
5	118,224	70,481	89,261	NA	60,880	73,794	21,626	NA
6	110,483	28,029	22,649	26,037	74,933	13,222	15,120	NA
7	24,860	5,270	17,782	50,260	240,819	18,978	13,667	NA
8	8,616	4,646	9,364	18,648	110,624	7,542	61,540	NA
9	11,709	3,115	11,275	32,598	216,233	14,757	7,892	NA
10	20,040	3,690	11,410	41,648	210,192	9,570	20,445	NA
11	1,699	34,993	11,115	115	167,196	6,338	16,803	39,591
12	3,428	87,840	6,072	1,654	217,711	91,775	132,668	60,479
13	615	120,462	2,251	227	130,624	6,996	193,519	49,262
14	3,399	157,473	2,255	1,050	165,636	6,009	217,976	65,532
15	154	77,993	1,572	11	36,696	1,525	43,027	54,593
16	6,770	1,602	36,154	3,425	292,973	NA	54,796	NA
17	13,230	816	60,832	14,227	226,466	NA	34,325	NA
18	4,816	2,211	37,700	2,563	189,211	NA	188,085	NA
19	3,300	507	42,414	1,670	86,353	NA	153,551	NA
20	20,017	3,741	17,922	5,347	106,887	NA	63,708	NA
21	2,020	1,038	37,139	785	201,874	NA	141,531	NA

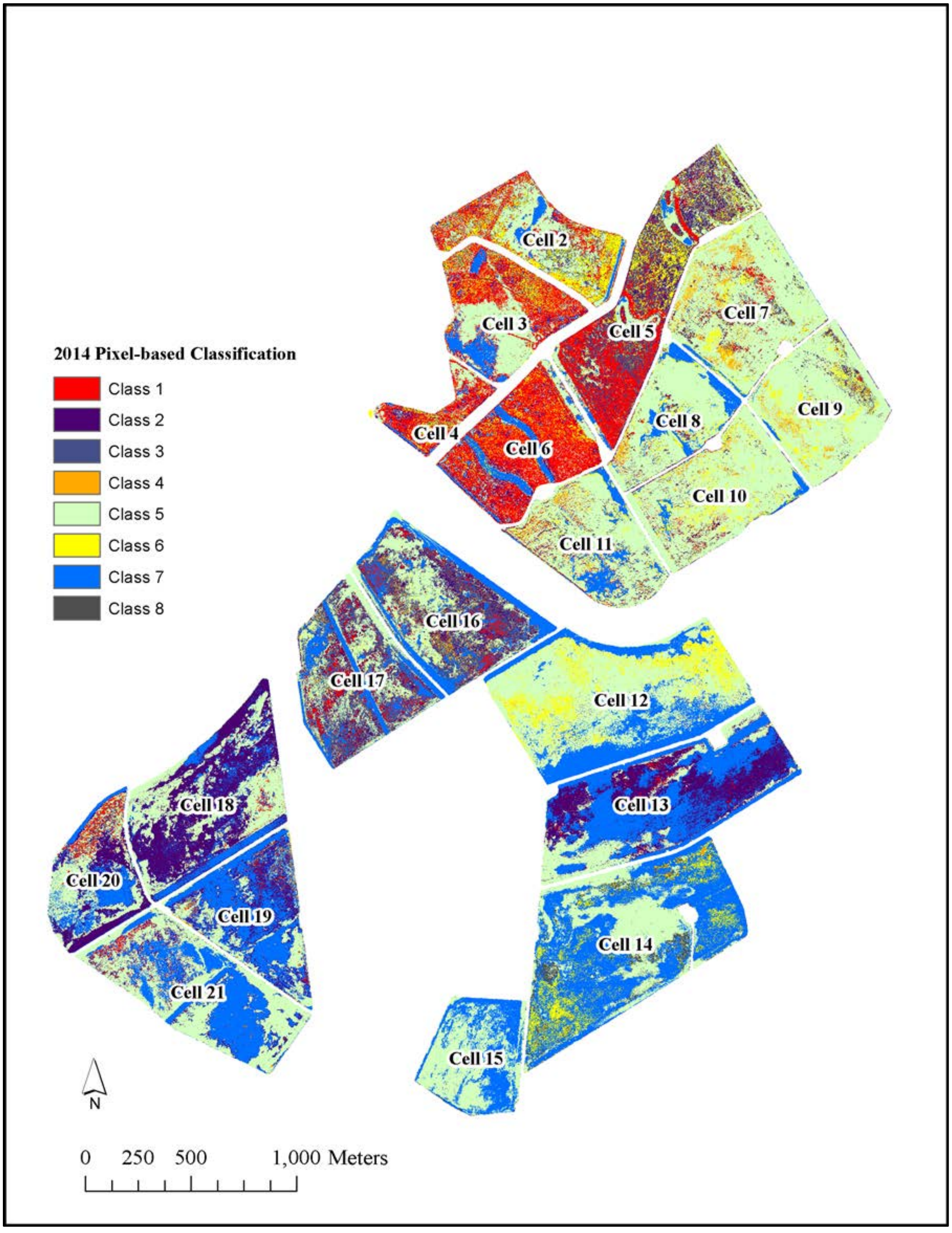

Figure 2. 2014 Pixel-based classification

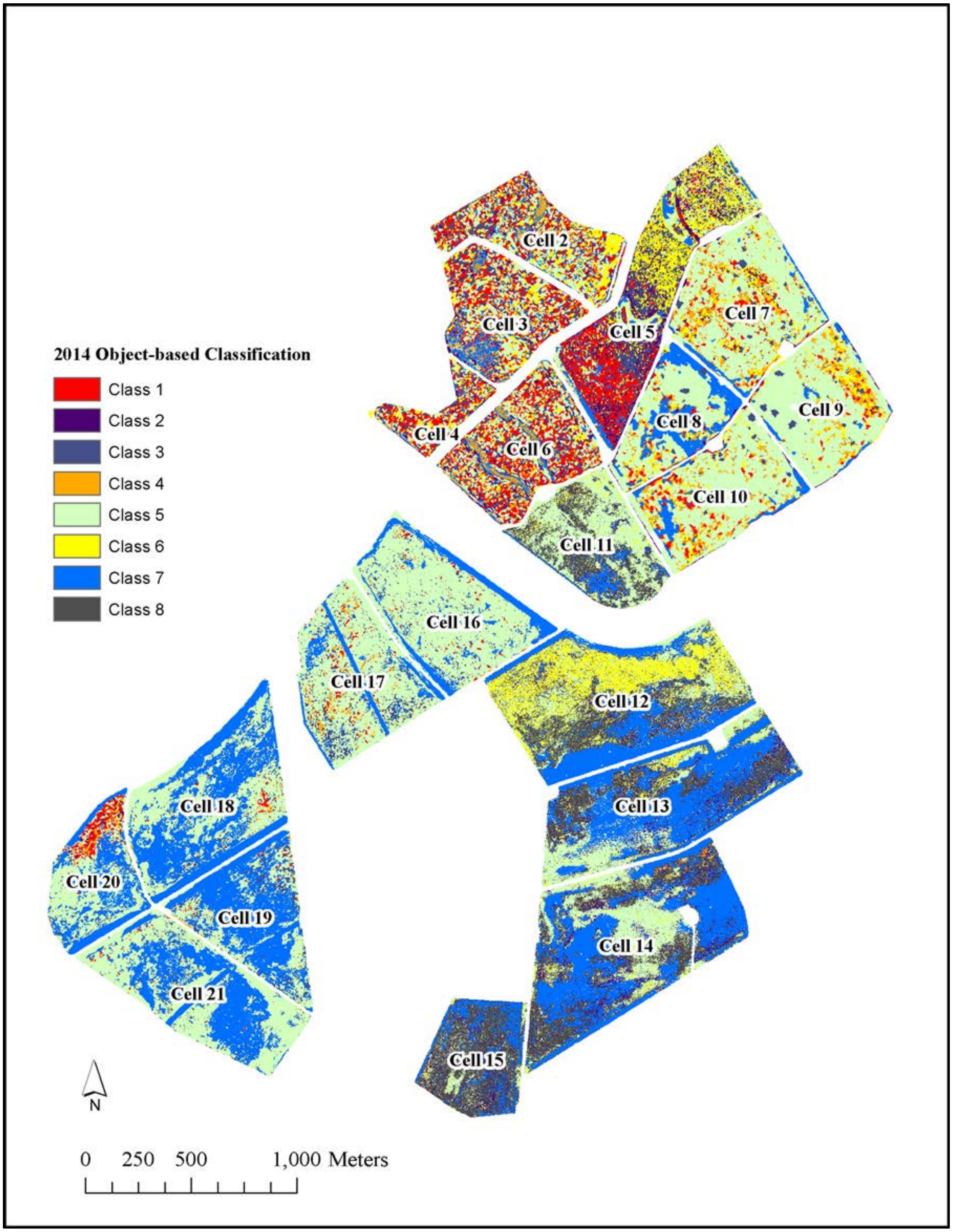

Figure 3. 2014 Object-based classification

4.2 Accuracy results of 2014 PBSIA and OBIA classifications

The accuracy of both classification methods was assessed using accuracy reports generated in ERDAS Imagine. The pixel-based method resulted in an overall classification accuracy of 43.33% (Table 5). Most class specific accuracies were poor as the overall accuracy indicates, but a few classes produced accuracies of moderate agreement (Table 5). Classes with moderate agreement include Class 5 (Algae/Pondweed/Duckweed), which resulted in a producer's accuracy of 61%, as well as a user's accuracy of 67% (Table 5). Class 7 (Open water/Submerged) also demonstrated moderate agreement with producer's and user's accuracy at 78% and 60%, respectively (Table 5). Class 8 (American Lotus/Primrose) also resulted in moderate agreement as producer's and user's accuracies were both approximately 60% (Table 5). Class 1 (Cattail) provided poor agreement with producer's and user's accuracies just below 50% (Table 5). The outcome for Class 2 (Bullrush/Burhead/Toothcup) exhibited even less agreement, with producer's and user's accuracies of 28% and 27%, respectively (Table 5). Class 3 (Spikerush/Sedge) resulted in the lowest accuracies with extremely poor producer's (8%) and user's (10%) accuracies (Table 5).

The object-based classification yielded an overall classification accuracy of 62.92% and demonstrated a stronger agreement between reference and classified objects for all classes (Table 6). Class 1 (Cattail) showed strong agreement with a producer's accuracy of nearly 83% and a user's accuracy of 80% (Table 6). Classes 2, 6, 7 and 8 indicated moderately strong agreement with producer's accuracies just under 70% (Table 6). Class 5 resulted in a producer's accuracy of 59% and a user's accuracy of 67% (Table

6). Class 4 (Arrowhead) indicated a weak agreement with producer's and user's accuracies of 40% (Table 6).

Kappa coefficient of agreement statistics further support the strong agreement of the OBIA classification as demonstrated in the accuracy assessment report (Table 7). The overall Kappa statistic of 0.5762 indicates moderate agreement for the object-based classification, while a value of 0.324 for the PBSIA classification indicates poor agreement and unreliable accuracy revealed in the initial accuracy report (Table 7). The object-based conditional Kappa of 0.3208 for Class 4 (Arrowhead) is the only value that indicates weak agreement (Table 7). Other OBIA conditional Kappa's all indicate moderate to very strong agreement, including a value of 0.7725 for Class 1 (Cattail) (Table 7). The pixel-based Kappa conditional for Class 3 (Spikerush/Sedge), -0.064, demonstrates a complete lack of agreement and unreliable accuracy of the PBSIA classification for that class (Table 7).

Based on these accuracy outcomes of the classification methods used on the UAS imagery acquired in 2014, the object-based method was identified as the more accurate method to be used to classify the UAS imagery acquired in 2015 (Tables 5, 6, and 7).

Table 5. Accuracy results for pixel-based classification of UAS imagery acquired in 2014

2014 Pixel-based Classification Accuracy Results

Class Number and Name	Reference Totals	Classified Totals	# Correct	Producer's Accuracy	User's Accuracy
1 Cattail	29	30	14	48.28%	46.67%
2 Bulrush/Burhead/Toothcup	29	30	8	27.59%	26.67%
3 Spikerush/Sedge	37	30	3	8.11%	10.00%
4 Arrowhead	38	30	12	31.58%	40.00%
5 Algae/Duckweed/Pondweed	33	30	20	60.61%	66.67%
6 Smartweed/Barnyard/Millet	21	30	11	52.38%	36.67%
7 Open Water/Submerged	23	30	18	78.26%	60.00%
8 Am. Lotus/Primrose	30	30	18	60.00%	60.00%
Totals	240	240	104		

Overall Classification Accuracy = 43.33%

Table 6. Accuracy results for object-based classification of UAS imagery acquired in 2014

2014 Object-based Classification Accuracy Results

Class Name	Reference Totals	Classified Totals	# Correct	Producer's Accuracy	User's Accuracy
1 Cattail	29	30	24	82.76%	80.00%
2 Bulrush/Burhead/Toothcup	32	30	21	65.63%	70.00%
3 Spikerush/Sedge	32	30	17	53.13%	56.67%
4 Arrowhead	28	30	12	42.86%	40.00%
5 Algae/Duckweed/Pondweed	34	30	20	58.82%	66.67%
6 Smartweed/Barnyard/Millet	25	30	17	68.00%	56.67%
7 Open Water/Submerged	34	30	23	67.65%	76.67%
8 Am. Lotus/Primrose	26	30	17	65.38%	56.67%
Totals	240	240	151		

Overall Classification Accuracy = 62.92%

Table 7. Kappa statistic results for pixel-based and object-based classification of UAS imagery acquired in 2014

2014 UAV Imagery Classification KAPPA (K^) Statistics		
	Pixel-based	Object-based
Overall Kappa Statistics	**0.3524**	**0.5762**
Conditional Kappa for each Category		
Class Name	***Kappa***	***Kappa***
1 Cattail	0.3934	0.7725
2 Bulrush/Burhead/Toothcup	0.1659	0.6538
3 Spikerush/Sedge	-0.064	0.5
4 Arrowhead	0.2871	0.3208
5 Algae/Duckweed/Pondweed	0.6135	0.6117
6 Smartweed/Barnyard/Millet	0.3059	0.5163
7 Open Water/Submerged	0.5576	0.7282
8 Am. Lotus/Primrose	0.5429	0.514

4.3 2015 UAS imagery classification results

Object-based classification was used to classify the UAS imagery acquired in 2015. To assess the annual variations of wetland vegetation cover, the 2014 and 2015 object-based classifications were compared in a post-classification change detection.

The 2015 object-based classification yielded a total area of 531,054 m^2 for Class 1 (Cattail), 2,014,366 m^2 for Class 2 (Bulrush/Burhead/Toothcup), 314,405 m^2 for Class 3 (Spikerush/Sedge), 686,916 m^2 for Class 4 (Arrowhead), and 312,498 m^2 for Class 5 (Algae/Duckweed/Pondweed) (Table 9). 2015 area totals also include 555,113m^2 of Class 6 (Smartweed/Barnyard Grass/ Millet), 2,121,975m^2 of Class 7 (Open Water/Submerged), 503,977m^2 of Class 8 (American Lotus/Primrose), 46,412 m^2 of Class 9 (Sesbania/Button Bush), and 24,377 m^2 of Class 10 (Ash Tree) (Figure 4) (Table 9).

Table 8. Total area (m²) results for object-based classification of UAS imagery acquired in 2015

2015 Total Area (m²) of Object-based Classification	
Class # Class Name	**Total Area (m²)**
1 Cattail	1,276,529
2 Bulrush/ Burhead/ Toothcup	2,014,366
3 Spikerush/ Sedge	314,405
4 Arrowhead	686,916
5 Algae/ Duckweed/ Pondweed	312,498
6 Smartweed/ Barnyard Grass/ Millet	555,113
7 Open Water/ Submerged	2,121,975
8 Am. Lotus/ Primrose	503,977
9 Sesbania/ Button Bush	46,412
10 Ash Tree	24,377

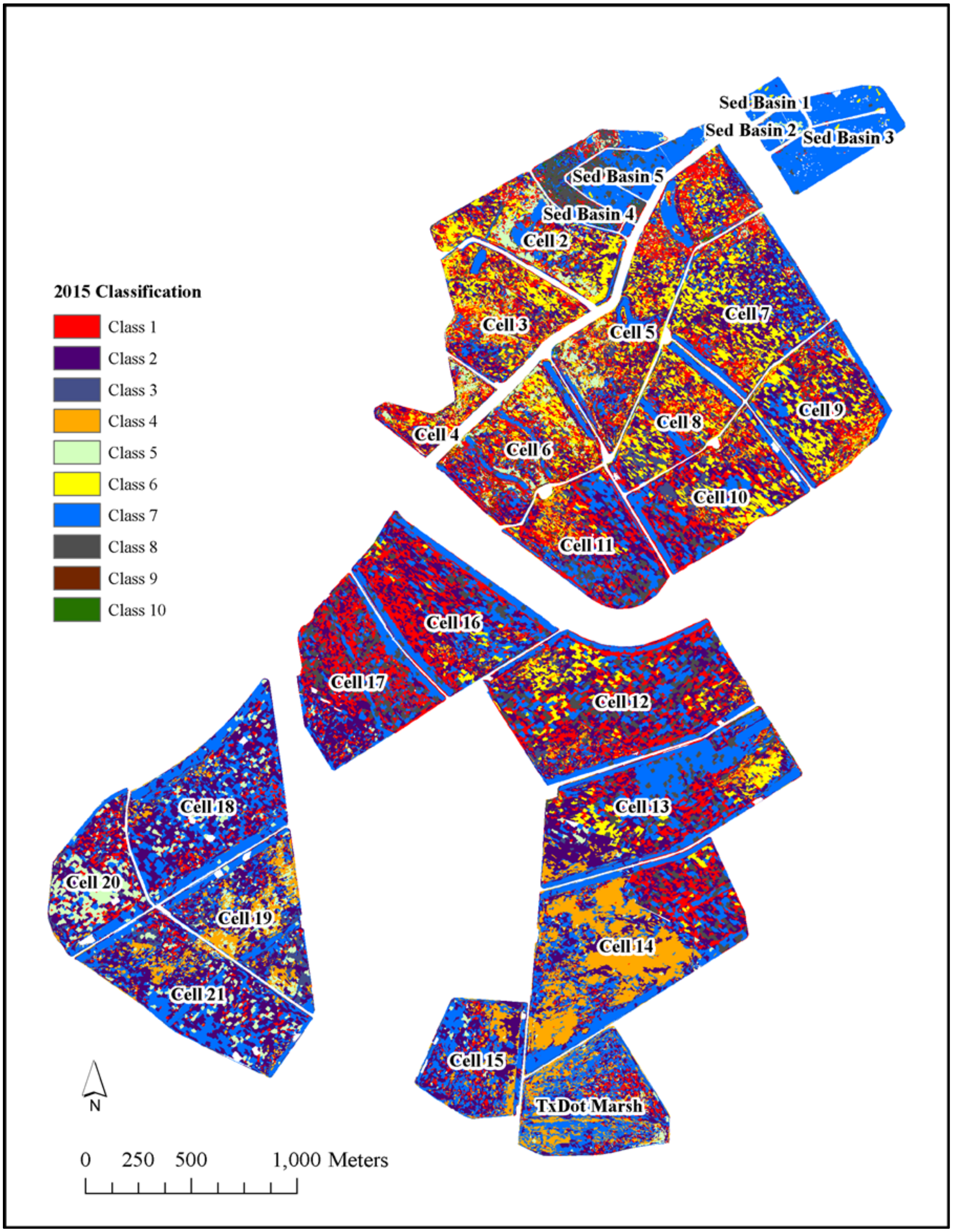

Figure 4. 2015 Object-based classification

4.4 Accuracy results of 2015 classification

The 2015 object-based classification yielded a poor overall classification accuracy of 29.00% and demonstrated weak agreement between reference and classified objects for all classes (Table 9). Class 1 (Cattail) showed weak agreement with a producer's accuracy of 13.73% and a user's accuracy of 23.33% (Table 9). Classes 2 (Bulrush/Burhead/Tootchup) indicated weak agreement with a producer's accuracy of 13.89% and a user's accuracy of 16.67% (Table 9). Class 5 (Algae/Duckweed/Pondweed) resulted in better accuracy with a user's accuracy of 50% (Table 9). Class 4 (Arrowhead) also demonstrated more moderate agreement with a producer's accuracy of 40% (Table 9). Class 7 (Open Water/Submerged) demonstrated the highest user's accuracy at 53.33% and Class 9 (Sesbania/Button Bush) demonstrated the poorest user's accuracy at 6.67%

Kappa coefficient of agreement statistics further indicated the weak agreement of the 2015 object-based classification with an overall kappa statistic of 0.2111 (Table 10). The highest conditional Kappa's were 0.4253 for Class 5 (Algae/Duckweed/Pondweed) and 0.4553 for Class 7 (Open Water Submerged) (Table 10). The weakest conditional Kappa's were 0.053 for Class 2 (Bulrush/Burhead/Toothcup) and 0.0244 for Class 9 (Sesbania/Button Bush) (Table 10).

Table 9. Accuracy results for object-based classification of UAS imagery acquired in 2015

2015 Object-based Classification Accuracy Results					
Class Name	**Reference Totals**	**Classified Totals**	**# Correct**	**Producer's Accuracy**	**User's Accuracy**
1 Cattail	51	30	7	13.73%	23.33%
2 Bulrush/Burhead/Toothcup	36	30	5	13.89%	16.67%
3 Spikerush/Sedge	24	30	9	37.50%	30.00%
4 Arrowhead	25	30	10	40.00%	33.33%
5 Algae/Duckweed/Pondweed	39	30	15	38.46%	50.00%
6 Smartweed/Barnyard /Millet	36	30	10	27.78%	33.33%
7 Open Water/Submerged	43	30	16	37.21%	53.33%
8 Am. Lotus/Primrose	30	30	10	33.33%	33.33%
9 Sesbania/Button Bush	13	30	2	15.38%	6.67%
10 Ash Tree	3	30	3	100.00%	10.00%
Totals	300	300	87		
Overall Classification Accuracy = 29.00%					

Table 10. Kappa statistic results for object-based classification of UAS imagery acquired in 2015

2015 Classification KAPPA (K^) Statistics	
Overall Kappa Statistics	**0.2111**
Conditional Kappa for each Category	
Class Name	***Kappa***
1 Cattail	0.0763
2 Bulrush/Burhead/Toothcup	0.053
3 Spikerush/Sedge	0.2391
4 Arrowhead	0.2727
5 Algae/Duckweed/Pondweed	0.4253
6 Smartweed/Barnyard /Millet	0.2424
7 Open Water/Submerged	0.4553
8 Am. Lotus/Primrose	0.2593
9 Sesbania/Button Bush	0.0244
10 Ash Tree	0.0909

4.5 Change detection results of 2014 and 2015 classifications

Analysis was concluded with a post classification change detection between the 2014 and 2015 object-based classifications, despite the poor accuracy yielded by the 2015 classification. The 2015 classification included additional areas of RCWMA as requested by management, however, these areas were excluded from the change detection as they were not classified for 2014.

From 2014 to 2015, 23% of Class 1 (Cattail) was unchanged and 22% transitioned to Class 2 (Bulrush/Burhead/Toothcup) (Table 11). Twenty seven percent of Class 2 remained Class 2 and 19% transitioned to Class 1 by 2015 (Table 12). Nearly 21% of Class 3 (Spikerush/Sedge) transitioned to Class 1 and almost 30% transitioned to Class 2 according to the 2015 classification (Table 13). Class 4 (Arrowhead) also experienced similar differences as transition included 23 % for Class 1 and 26% for Class 2 (Table 14). For Class 5 (Algae/Duckweed/Pondweed) transition included a nearly 30% shift to Class 2, as well as 21% to Class 8 (Open Water/Submerged) (Table 15). Class 6 (Smartweed/Barnyard/Millet) underwent similar change as previously described for Classes 3 and 4 (Table 16). Class 7 (Open Water/Submerged) largely remained unchanged but also experienced a transition of 27% to Class 2 (Table 17). Class 8 (American Lotus/Primrose) experienced a 28% transition to Class 2 and a 23% transition to Class 8 (Table 18).

Table 11. Class 1 change detection results

Classified as Class 1 (Cattail) in 2014		
2015 Classification	%	Area (m^2)
Class 0 (Unclassified)	0	1,180
Class 1 (Cattail)	23.17	89,010
Class 2 (Bulrush/Burhead/Toothcup)	22.34	85,830
Class 3 (Spikerush/Sedge)	4.85	18,610
Class 4 (Arrowhead)	9.83	37,760
Class 5 (Algae/Duckweed/Pondweed)	8.11	31,160
Class 6 (Smartweed/Barnyard /Millet)	13.5	51,850
Class 7 (Open Water/Submerged)	9.34	35,870
Class 8 (Am. Lotus/Primrose)	5.6	21,530
Class 9 (Sesbania/Button Bush)	2.69	10,320
Class 10 (Ash Tree)	0.58	2,230
Total	100	384,180

Table 12. Class 2 change detection results

Classified as Class 2 (Bulrush/Burhead/Toothcup) in 2014		
2015 Classification	%	Area (m^2)
Class 0 (Unclassified)	0	2,430
Class 1 (Cattail)	18.95	56,220
Class 2 (Bulrush/Burhead/Toothcup)	26.79	79,450
Class 3 (Spikerush/Sedge)	3.36	9,980
Class 4 (Arrowhead)	12.38	36,720
Class 5 (Algae/Duckweed/Pondweed)	3.8	11,290
Class 6 (Smartweed/Barnyard /Millet)	7.53	22,350
Class 7 (Open Water/Submerged)	18.27	54,180
Class 8 (Am. Lotus/Primrose)	7.44	22,060
Class 9 (Sesbania/Button Bush)	1.12	3,330
Class 10 (Ash Tree)	0.36	1,060
Total	100	296,630

Table 13. Class 3 change detection results

Classified as Class3 (Spikerush/Sedge) in 2014		
2015 Classification	%	Area (m^2)
Class 0 (Unclassified)	0	2,440
Class 1 (Cattail)	20.78	71,500
Class 2 (Bulrush/Burhead/Toothcup)	28.54	98,190
Class 3 (Spikerush/Sedge)	4.99	17,170
Class 4 (Arrowhead)	7.59	26,110
Class 5 (Algae/Duckweed/Pondweed)	5.19	17,870
Class 6 (Smartweed/Barnyard /Millet)	11.99	41,270
Class 7 (Open Water/Submerged)	13.75	47,320
Class 8 (Am. Lotus/Primrose)	5.84	20,110
Class 9 (Sesbania/Button Bush)	1.06	3,660
Class 10 (Ash Tree)	0.26	890
Total	100	344,090

Table 14. Class 4 change detection results

Classified as Class 4 (Arrowhead) in 2014		
2015 Classification	%	Area (m^2)
Class 0 (Unclassified)	0	840
Class 1 (Cattail)	22.5	56,320
Class 2 (Bulrush/Burhead/Toothcup)	26.36	65,980
Class 3 (Spikerush/Sedge)	4.38	10,960
Class 4 (Arrowhead)	6.47	16,190
Class 5 (Algae/Duckweed/Pondweed)	4.44	11,120
Class 6 (Smartweed/Barnyard /Millet)	13.1	32,800
Class 7 (Open Water/Submerged)	15.16	37,950
Class 8 (Am. Lotus/Primrose)	5.63	14,090
Class 9 (Sesbania/Button Bush)	1.48	3,690
Class 10 (Ash Tree)	0.48	1,190
Total	100	250,290

Table 15. Class 5 change detection results

Classified as Class 5 (Algae/Duckweed/Pondweed) in 2014		
2015 Classification	%	Area (m²)
Class 0 (Unclassified)	0	13,430
Class 1 (Cattail)	18.11	527,580
Class 2 (Bulrush/Burhead/Toothcup)	29.64	863,540
Class 3 (Spikerush/Sedge)	4.4	128,260
Class 4 (Arrowhead)	7.35	214,070
Class 5 (Algae/Duckweed/Pondweed)	3.88	113,170
Class 6 (Smartweed/Barnyard /Millet)	8.67	252,510
Class 7 (Open Water/Submerged)	21.39	623,140
Class 8 (Am. Lotus/Primrose)	5.93	172,920
Class 9 (Sesbania/Button Bush)	0.48	13,900
Class 10 (Ash Tree)	0.16	4,730
Total	100	2,913,820

Table 16. Class 6 change detection results

Classified as Class 6 (Smartweed/Barnyard /Millet) in 2014		
2015 Classification	%	Area (m²)
Class 0 (Unclassified)	0	2,450
Class 1 (Cattail)	21.49	93,250
Class 2 (Bulrush/Burhead/Toothcup)	24.03	104,270
Class 3 (Spikerush/Sedge)	5.29	22,940
Class 4 (Arrowhead)	5.98	25,970
Class 5 (Algae/Duckweed/Pondweed)	2.25	9,780
Class 6 (Smartweed/Barnyard /Millet)	17.03	73,890
Class 7 (Open Water/Submerged)	14	60,770
Class 8 (Am. Lotus/Primrose)	8.94	38,800
Class 9 (Sesbania/Button Bush)	0.76	3,320
Class 10 (Ash Tree)	0.21	900
Total	100	433,880

Table 17. Class 7 change detection results

Classified as Class 7 (Open Water/Submerged) in 2014		
2015 Classification	%	Area (m^2)
Class 0 (Unclassified)	0	14,530
Class 1 (Cattail)	11.81	196,590
Class 2 (Bulrush/Burhead/Toothcup)	27.03	449,860
Class 3 (Spikerush/Sedge)	3.03	50,460
Class 4 (Arrowhead)	9.13	152,000
Class 5 (Algae/Duckweed/Pondweed)	5.17	86,110
Class 6 (Smartweed/Barnyard /Millet)	2.54	42,240
Class 7 (Open Water/Submerged)	35.63	593,050
Class 8 (Am. Lotus/Primrose)	5.33	88,730
Class 9 (Sesbania/Button Bush)	0.26	4,390
Class 10 (Ash Tree)	0.06	1,070
Total	100	1,664,490

Table 18. Class 8 change detection results

Classified as Class 8 (Am. Lotus/Primrose) in 2014		
2015 Classification	%	Area (m^2)
Class 0 (Unclassified)	0	2,070
Class 1 (Cattail)	15.78	95,410
Class 2 (Bulrush/Burhead/Toothcup)	28.24	170,780
Class 3 (Spikerush/Sedge)	3.18	19,200
Class 4 (Arrowhead)	15.61	94,360
Class 5 (Algae/Duckweed/Pondweed)	0.81	4,900
Class 6 (Smartweed/Barnyard /Millet)	4.09	24,760
Class 7 (Open Water/Submerged)	23.43	141,650
Class 8 (Am. Lotus/Primrose)	8.59	51,960
Class 9 (Sesbania/Button Bush)	0.24	1,450
Class 10 (Ash Tree)	0.03	170
Total	100	604,640

5.0 DISCUSSION

5.1 UAS Classification of Vegetation

The UAS imagery utilized in this research permitted the production of a wetland vegetation cover dataset at a high spatial resolution (16-18 cm) for both 2014 and 2015. However, low altitude data acquisition limited the footprint size and the total area each individual image covered. This reduction in footprint size, similar to the study conducted by Jensen et al. (2011), required the majority of time be dedicated to extensive processing and geo-referencing tasks.

In addition, when using a UAS to acquire imagery, limited footprint size also delays and complicates classification performance when surveying a large-scale site due to the time sensitive limitations related to variation in lighting conditions. Imagery acquired in 2014 was divided into four separate flights which provided overlap over certain cells and wetland area. This required pre-processing of not only four RGB mosaics, but four NIR mosaics as well, in addition to ensuring that the corresponding RGB and NIR mosaics aligned precisely. Despite these complications, this research outlines an innovative procedure for effective monitoring and classification of a large-scale site, while the majority of UAS classification of vegetation studies are conducted over minor areas (Semeraro et al. 2015, Masi et al. 2013)..

The results of this research support the conclusions of other UAS vegetation classification studies, including Lehman et al.'s (2015) detection of pest infestation on a branch level utilizing object specific features, which demonstrates the evolving proficiencies of object-based methods and high-resolution UAS imagery. By addressing vegetation classes independently, the object-based classification was able to implement background user knowledge, also an advantage reinforced by Lehman's et al. (2015) OBIA vegetation classification. For example, the tendency of Class 1 (Cattail) to form in adjacent circular clumps was accounted for in the classification by including elliptical fit and shape index as a primary weighted feature employed to identify Class 1.

The accuracy outcomes of the 2014 object-based classification established high accuracy standards for large-scale classification of wetland vegetation using high-resolution UAS imagery. The reliability of the 2014 dataset is comparable to existing research regarding vegetation classification at high spatial resolution (Desclée et al. 2006; Yu et al. 2006). The superior results of the 2014 object-based classification support the findings outlined in comparative vegetation classification studies conducted by Desclée et al. (2006), Yu et al. (2006), Mantifar et al. (2007), Conchedda et al. (2008), and Dronova et al. (2012). Supported findings include evidence that object-based classification offers alternative means to address the complex and heterogeneous nature of wetlands, improve overall classification accuracy, and prevent production of the "salt-and-pepper effect".

5.2 Influence of Classification Method on Outcomes

These results demonstrate that object-based classification can provide outputs where the effect of interspersed, fine spatial scale vegetation mixing is mitigated. Traditional pixel-based classification is efficient and straightforward as opposed to object-based classification, which required dedication of more time for processing tasks, algorithm modifications, and general demand of user input. Object-based classification can fully utilize background user knowledge by readily applying spatial concepts to the classification approach (Benz et al. 2004). By including contextual information, rather than only spectral information, object-based classification offers the opportunity to maximize accuracy and minimize the likelihood of producing results significantly affected by the "salt-and-pepper effect." However, the initial segmentation of imagery into objects does not always prevent the "salt-and-pepper effect" (Blaschke 2010). If the user does not utilize the appropriate segmentation approach and apply suitable spatial information to the classification, spectral characteristics of image objects may produce the "salt-and-pepper effect" only at a larger minimum mapping unit (Matinfar et al. 2007).

The minimum mapping unit or unit of analysis is important to consider when comparing the two classification methods used in this research. As previously verified in a study conducted by Baker et al. (2007), defining classification parameters with high spatial resolution is delicate when detecting pattern differences in heterogeneous wetland areas, and careful assessment of the minimum mapping unit is crucial. For the purposes of this research, the unit of analysis for the pixel-based classification was defined, by default, as the spatial resolution of the imagery or the size of the pixel. The object-based classification defines the unit of analysis depending on the scale parameter used for the segmentation process and is generally larger than the size of a pixel. Therefore, the segmentation step of OBIA can potentially mitigate this issue before classification has even begun (Mantifar et al. 2007). Alternatively, if the segmentation is performed with little scrutiny of the minimum mapping unit, this step could inversely increase the odds of producing the "salt-and-pepper effect" among larger units of analysis (Conchedda et al. 2008). However, as demonstrated by Dronova et al. (2012), who tested segmentation scale suitability for the classification of six plant functional type families, it is possible that none of the segmentation scales offer any measurable advantage over the others.

Another notable consideration when comparing PBSIA and OBIA is the difference in the classification algorithm used. While OBIA methods can employ a nearly endless combination of classification algorithms to a weighted variety of vegetation classes, the PBSIA classification presented in this research utilized a single nearest neighbor classification algorithm applied to five bands of data.

More importantly, an extensive amount of time was dedicated to the object-based classification in order to test variations of segmentation and alter the classification algorithm, sometimes up to three or four times. If a similar amount of time was devoted to the PBSIA classification through additional post-processing techniques like application of a low pass-filter, accuracy of the pixel-based results may have been enhanced (Walter 2000). Because significantly more time was committed to the object-based classification and a minimal amount of time to the pixel-based classification, these results may reflect this difference in time spent as shown in a comparative study completed by Yu et al. (2006), and therefore may serve as a source of error and uncertainty.

5.3 Sources of Error and Uncertainty

As mentioned previously, the small footprint size of the imagery acquired in 2014 required the study area to be separated into four individual image mosaics, and as a result, in tandem with the time sensitive characteristics of UAS imagery collection, created classification complexities and challenges. These complexities should be considered as a potential source of error and uncertainty as ground truth data was collected inconsistently throughout the four flights. Ground truth data collection was conducted under the assumption that spectral signatures of vegetation classes from one cell or individual flight could be used to classify the vegetation class for the entire area. However, as the imagery was collected at different times of day, with varying cloud cover conditions, and some cells were individually classified, this option was not feasible and required some improvisation through visual interpretation. Additionally, some classes were simply challenging to classify because of the lack of ground truth data for cells imaged during different flights.

The 2015 object-based results exhibit poor, unreliable accuracy, and is largely the consequence of classifying imagery collected under less than ideal acquisition conditions. Under these acquisition conditions, an enhanced payload that should have allowed imagery of the entire study area to be collected in two flights, instead required the collection of imagery in four flights. All four flights were acquired under dissimilar illumination conditions and cloud cover, ultimately requiring twice the amount of processing and georefrencing time simply to determine which imagery would be most reliable for the classification. Due to inconsistent illumination conditions, three out of the four flights resulted in extremely dark imagery, only usable in the middle section of the mosaic. Consequently, three mosaics, all acquired from different flights were necessary for classification of the entire study area.

In addition, partial cloud cover created spectral inconsistency, prevented uniform segmentation, and complicated adequate separation of classes. The poor accuracy of the 2015 classification also limits the value of performing an annual change detection from 2014 to 2015. While the purpose of this research was to assess the accuracy of classification methods, the 2015 classification results and annual change detection for this study area and the time period of analysis would be of limited benefit to wetland managers.

6.0 CONCLUSION

6.1 Conclusion

UAS platforms provide an economical approach to acquire imagery with high temporal and spatial resolutions. UAS platforms are ideal for wetland and other natural resource managers because UAS image acquisition enables detailed species-level mapping to be conducted efficiently. Monitoring wetland vegetation is critical to assessing wetland health and productivity. To effectively assess the spatial complexities of wetland vegetation, species-level mapping should be completed once a year at minimum.

This research used GIS, remote sensing, and statistical analysis to assess the accuracy of pixel-based, and object-based classification methods for mapping of wetland vegetation with imagery acquired by UAS. The 2014 classification results indicate that object-based classification produced more accurate results than the pixel-based classification method. In addition, overall accuracy statistics demonstrate how these methods can produce drastically different results. Assessing these statistics at each individual cell also reveals the contrast between results of pixel-based and object-based classification.

In addition, the low accuracy of the 2015 classification was primarily due to the lack of image quality. These results demonstrate the importance of comprehensive mission planning and disciplined image acquisition. Thorough preparation of acquisition procedure can minimize processing complications related to time of day differences and contrast of lighting conditions. The potential accuracy of classification results can be maximized if multiple flights are conducted only under a strict protocol that guarantees practical compatibility of imagery.

APPENDIX SECTION

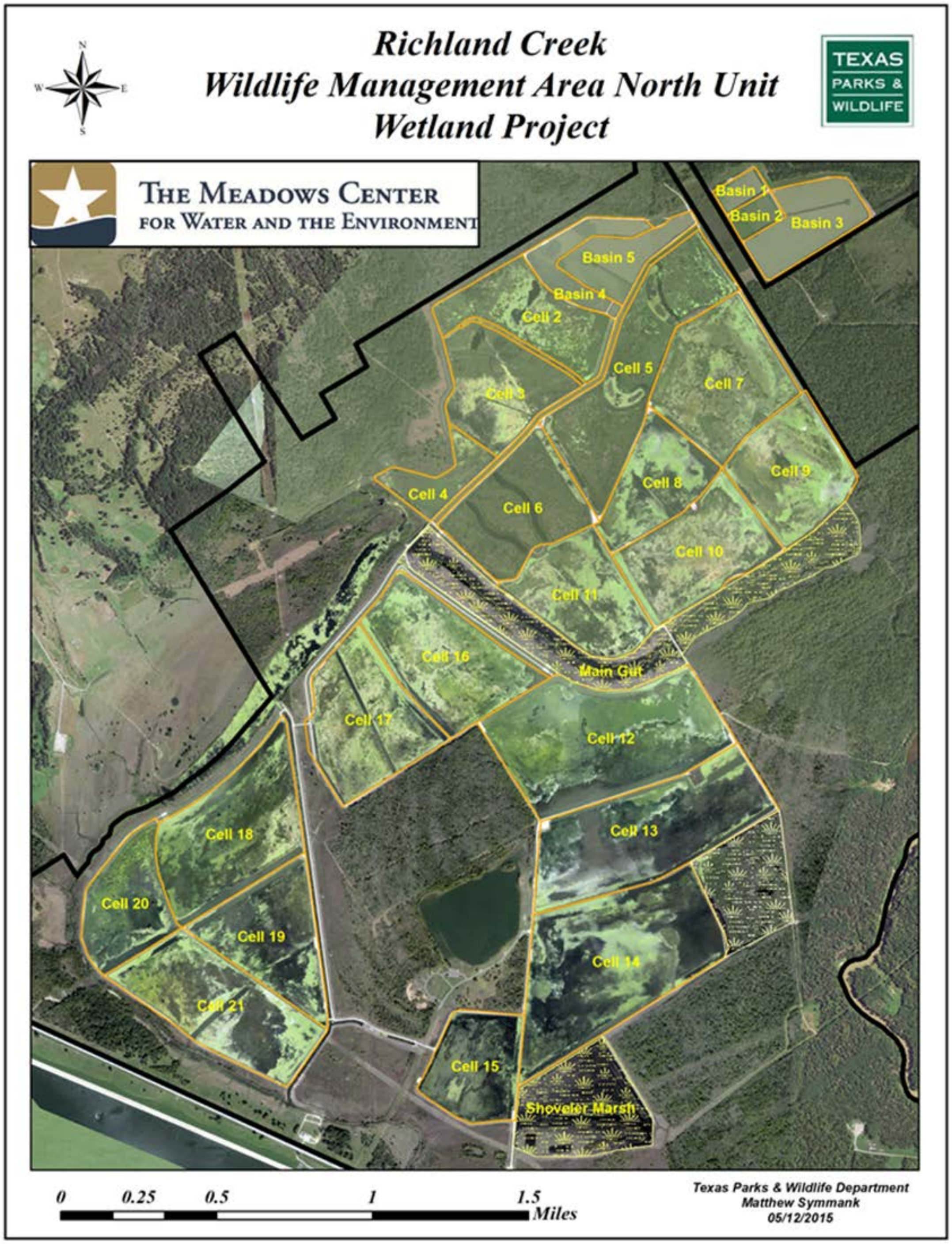

Figure 1. Study Area

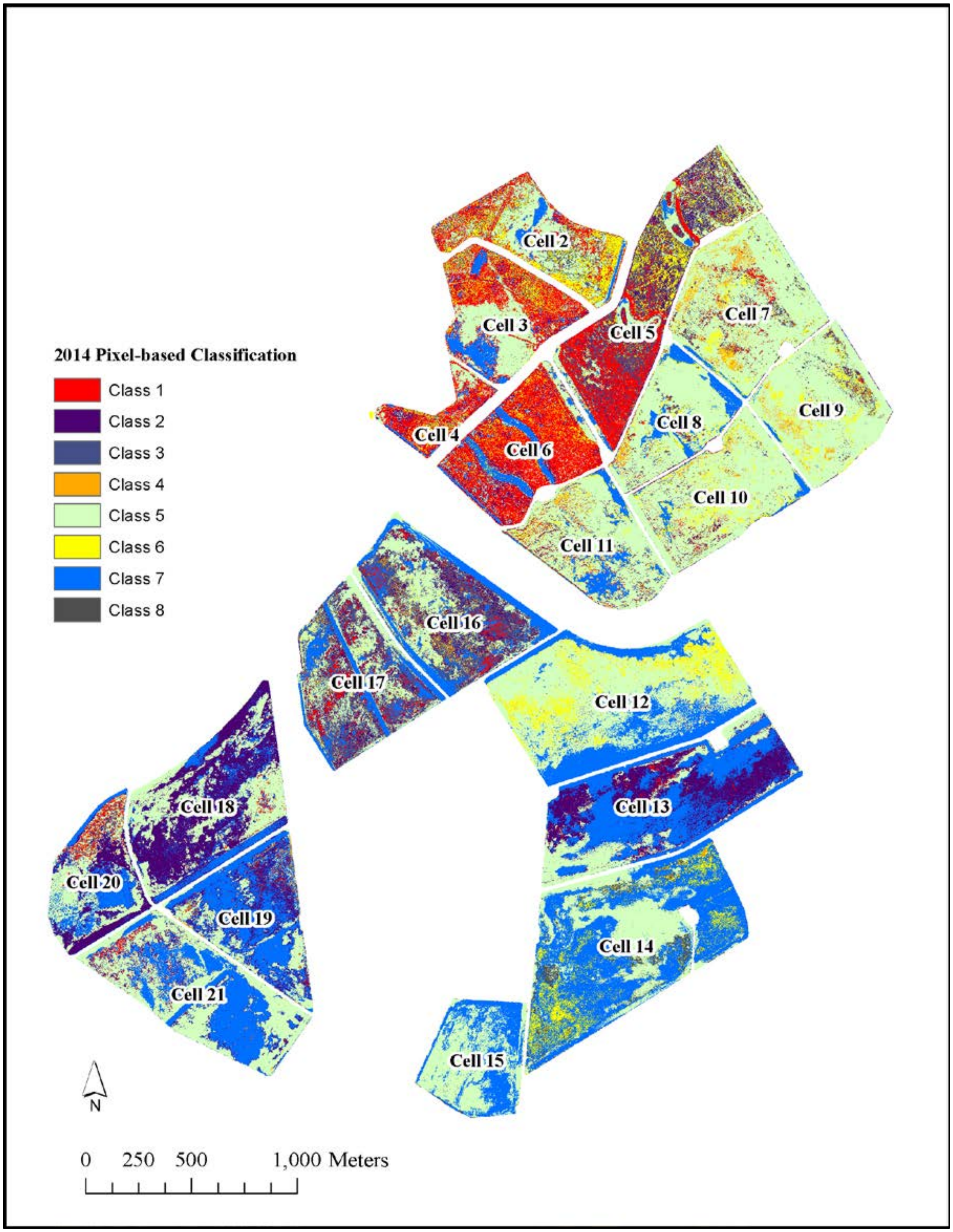

Figure 2. 2014 Pixel-based classification

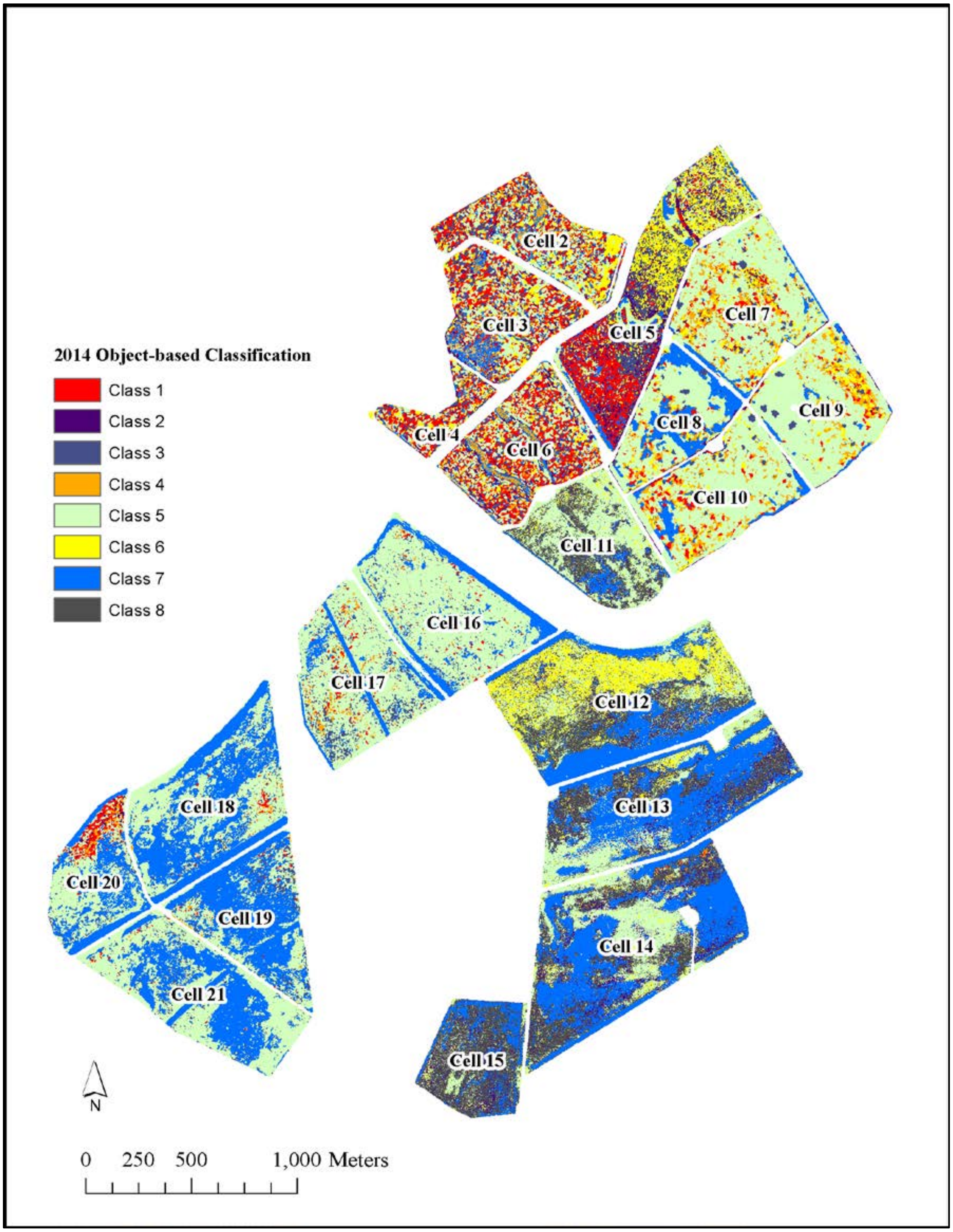

Figure 3. 2014 Object-based classification

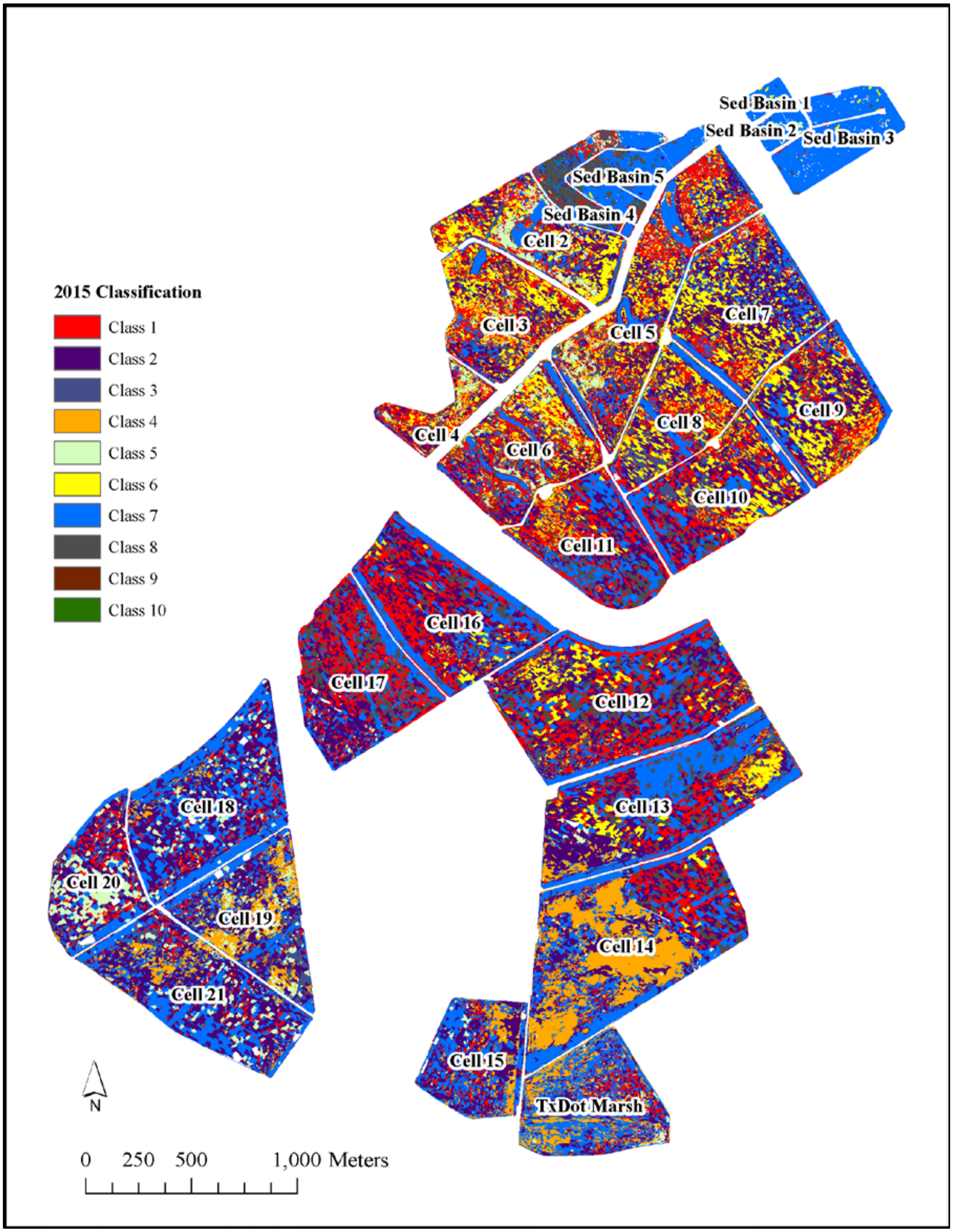

Figure 4. 2015 Object-based classification

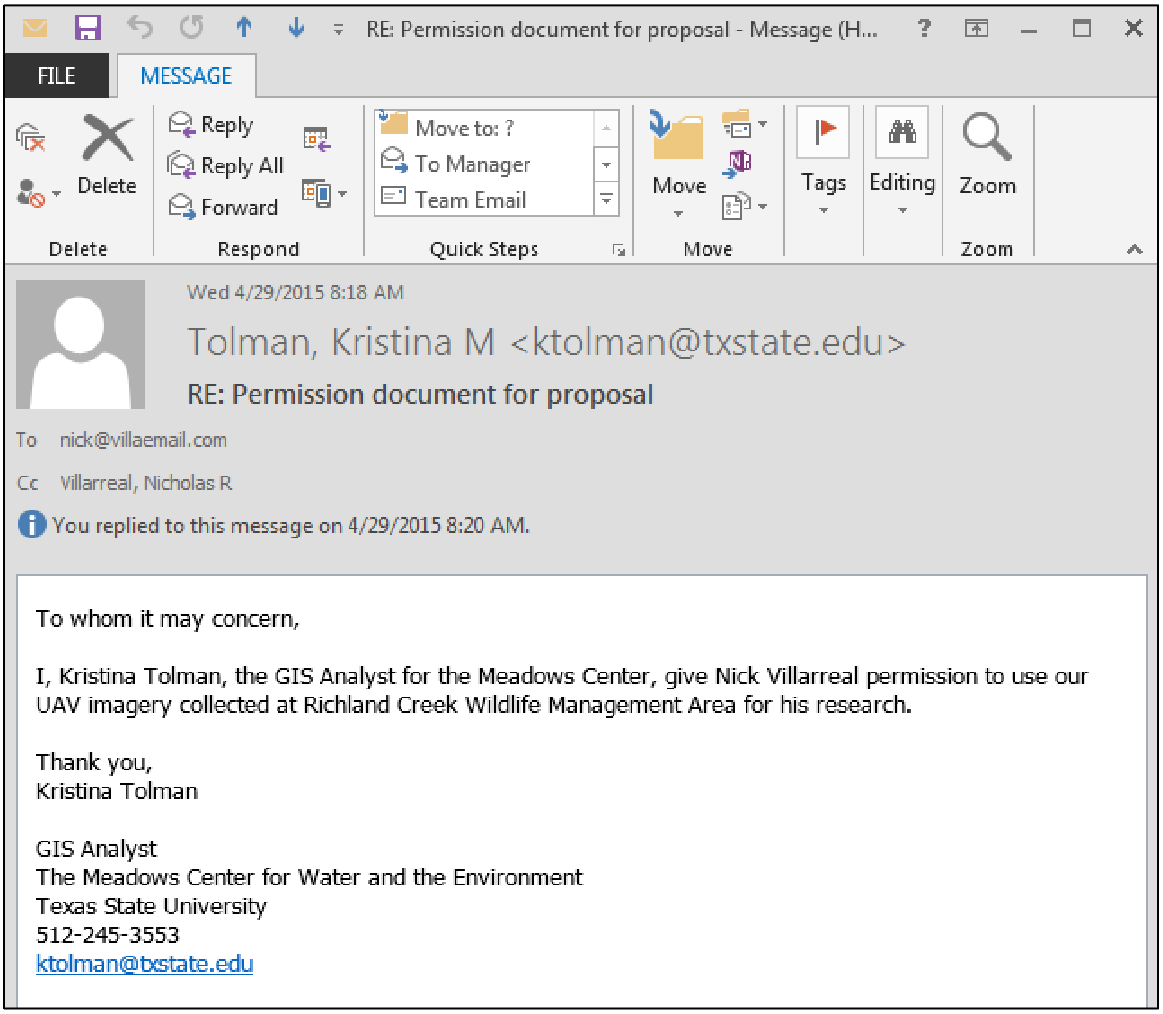
RE: Permission document for proposal - Message (H...

Wed 4/29/2015 8:18 AM

Tolman, Kristina M <ktolman@txstate.edu>

RE: Permission document for proposal

To nick@villaemail.com

Cc Villarreal, Nicholas R

You replied to this message on 4/29/2015 8:20 AM.

To whom it may concern,

I, Kristina Tolman, the GIS Analyst for the Meadows Center, give Nick Villarreal permission to use our UAV imagery collected at Richland Creek Wildlife Management Area for his research.

Thank you,
Kristina Tolman

GIS Analyst
The Meadows Center for Water and the Environment
Texas State University
512-245-3553
ktolman@txstate.edu

Figure 5. Permission to use data

WORKS CITED

Adam, Elhadi, Onisimo Mutanga, and Denis Rugege. "Multispectral and Hyperspectral Remote Sensing for Identification and Mapping of Wetland Vegetation: A Review." *Wetlands Ecology and Management* 18 (2010): 281–96.

Addink, Ea, Sm De Jong, and Ej Pebesma. "The Importance of Scale in Object-Based Mapping of Vegetation Parameters with Hyperspectral Imagery." *Photogrammetric Engineering & Remote Sensing* 73, no. 8 (2007): 905–12.

Baker, C., R. L. Lawrence, C. Montagne, and D. Patten. 2007. *Change Detection of Wetland Ecosystems Using Landsat Imagery and Change Vector Analysis.* WETLANDS, 27(3): 610 – 619.

Benz, Ursula C., Peter Hofmann, Gregor Willhauck, Iris Lingenfelder, and Markus Heynen. "Multi-Resolution, Object-Oriented Fuzzy Analysis of Remote Sensing Data for GIS-Ready Information." *ISPRS Journal of Photogrammetry and Remote Sensing* 58 (2004): 239–58.

Blaschke, T. "Object Based Image Analysis for Remote Sensing." *ISPRS Journal of Photogrammetry and Remote Sensing* 65, no. 1 (2010): 2–16.

Blaschke, Thomas, Stefan Lang, Eric Lorup, Josef Strobl, and Peter Zeil. "Object-Oriented Image Processing in an Integrated GIS / Remote Sensing Environment and Perspectives for Environmental Applications." *Umweltinformation Für Planung, Politik Und Öffentlichkeit / Environmental Information for Planning, Politics and the Public*, no. 1995 (2000): 555–70.

Carabell v. United States Army Corps of Eng'rs, 391 F.3d 704, 2004 U.S. App. LEXIS 24904 (6th Cir. Mich., 2004)

Clemens, Shannon. "Procedures for Correcting Digital Camera Imagery Acquired by the AggieAir Remote Sensing Platform" 2012 (2012): 58. http://digitalcommons.usu.edu/gradreports/186.

Conchedda, Giulia, Laurent Durieux, and Philippe Mayaux. "An Object-Based Method for Mapping and Change Analysis in Mangrove Ecosystems." *ISPRS Journal of Photogrammetry and Remote Sensing* 63 (2008): 578–89.

Desclée, Baudouin, Patrick Bogaert, and Pierre Defourny. "Forest Change Detection by Statistical Object-Based Method." *Remote Sensing of Environment* 102 (2006): 1–11.

Dronova, Iryna, Peng Gong, Nicholas E. Clinton, Lin Wang, Wei Fu, Shuhua Qi, and Ying Liu. "Landscape Analysis of Wetland Plant Functional Types: The Effects of Image Segmentation Scale, Vegetation Classes and Classification Methods." *Remote Sensing of Environment* 127 (2012): 357–69.

Dronova, Iryna, Peng Gong, and Lin Wang. "Object-Based Analysis and Change Detection of Major Wetland Cover Types and Their Classification Uncertainty during the Low Water Period at Poyang Lake, China." *Remote Sensing of Environment* 115, no. 12 (2011): 3220–36.

Ehlers, M, M Geehler, and R Janowsky. "Automated Techniques for Environmental Monitoring and Change Analyses for Ultra High Resolution Remote Sensing Data." *Photogrammetric Engineering and Remote Sensing* 72, no. 7 (2006): 835–44.

Fairbairn, S. E. and J.J Dinsmore. 2001. *Local and Landscape-Level Influences on Wetland Bird Communities of The Prairie Pothole Region of Iowa, USA.* WETLANDS, 21(1): 41-47.

Houck, Oliver A. "The Reckoning : Oil and Gas Development in the Louisiana Coastal Zone." *Tulane Environmental Law* 28, no. 2 (2015): 185–296.

Jensen, A. M. (2008). *Cooperative remote sensing for real-time water management and distributed irrigation control Band-reconfigurable Multi-UAV-based*, (January 2016).

Jensen, A.M., T. Hardy, M. Mckee and Yang Quan Chen 2011. *Using a multispectral autonomous unmanned aerial remote sensing platform (AggieAir) for riparian and wetlands applications.* Vancouver, BC: IEEE.

Kelly, Maggi, Karin a. Tuxen, and Diana Stralberg. "Mapping Changes to Vegetation Pattern in a Restoring Wetland: Finding Pattern Metrics That Are Consistent across Spatial Scale and Time." *Ecological Indicators* 11, no. 2 (2011): 263–73.

Lechner, a. M., a. Fletcher, K. Johansen, and P. Erskine. "Characterising Upland Swamps Using Object-Based Classification Methods and Hyper-Spatial Resolution Imagery Derived From an Unmanned Aerial Vehicle." *ISPRS Annals of Photogrammetry, Remote Sensing and Spatial Information Sciences* I– 4, no. September (2012): 101–6.

Lehmann, Jan, Felix Nieberding, Torsten Prinz, and Christian Knoth. "Analysis of Unmanned Aerial System-Based CIR Images in Forestry—A New Perspective to Monitor Pest Infestation Levels." *Forests* 6, no. 3 (2015): 594–612.

Lyon, J. G., D. Yuan, R. S. Lunetta, and C. D. Elvidge. *A Change Detection Experiment Using Vegetation Indices*. Photogrammetric Engineering & Remote Sensing, 64 (2): 143-150.

Masi, F, S Caffaz, and a Ghrabi. "Multi-Stage Constructed Wetland Systems for Municipal Wastewater Treatment." *Water Science and Technology : A Journal of the International Association on Water Pollution Research* 67, no. 7 (2013): 1590–98.

Matinfar, H. R., F. Sarmadian, S. K. Alavi Panah, and R. J. Heck. "Comparisons of Object-Oriented and Pixel-Based Classification of Land Use/Land Cover Types Based on Lansadsat7, Etm+ Spectral Bands (Case Study : Arid Region of Iran)." *American-Eurasian Journal of Agriculture and Environmental Science* 2, no. 4 (2007): 448–56.

Moffett, Kevan B., and Steven M. Gorelick. "Distinguishing Wetland Vegetation and Channel Features with Object-Based Image Segmentation." *International Journal of Remote Sensing* 34, no. February 2015 (2013): 1332–54.

Moreno-Mateos, David, Mary E. Power, Francisco A. Comín, and Roxana Yockteng. "Structural and Functional Loss in Restored Wetland Ecosystems." *PLoS Biology* 10 (2012).

Yu, Qian, Peng Gong, Nick Clinton, Greg Biging, Maggi Kelly, Dave Schirokauer. "Object based Detailed Vegetation Classification with Airborne High Spatial Resolution Remote Sensing Imagery." *Photogrammetric Engineering and Remote Sensing* 72, no. 7 (2006): 799–811.

Semeraro, Teodoro, Cosimo Giannuzzi, Leonardo Beccarisi, Roberta Aretano, Antonella De Marco, M Rita Pasimeni, Giovanni Zurlini, and Irene Petrosillo. “A Constructed Treatment Wetland as an Opportunity to Enhance Biodiversity and Ecosystem Services.” *Ecological Engineering* 82 (2015): 517–26.

Sghair, a, and F Goma. “Remote Sensing and GIS for Wetland Vegetation Study,” 2013. http://theses.gla.ac.uk/id/eprint/4581.

Silvestri, Sonia, Marco Marani, and Alessandro Marani. “Hyperspectral Remote Sensing of Salt Marsh Vegetation, Morphology and Soil Topography.” *Physics and Chemistry of the Earth* 28, no. 1–3 (2003): 15–25. 7065(03)00004-4.

Solid Waste Agency of Northern Cook County v. U.S. Army Corps of Engineers, 531 U.S. 159, 167, 121 S. Ct. 675, 148 L. Ed. 2d 576 *(2001)*

Symmank, Matthew. “Wetlands on Richland Creek Wildlife Management Area: Providing Water for Wildlife and People.” *Texas Parks and Wildlife Department*; (2013).

Tiner, Ralph W., Megan W. Lang, and V Klemas. 2015. *Remote sensing of wetlands: applications and advances*.

Trimble Germany GmbH “.TRIMBLE eCOGNITION, eCognition Developer: User Guide 9.1.” 2015, 1–265.

United States Department of Agriculture. “Plants Database,” 2016. http://plants.usda.gov/java/.

United States v. Rapanos, 376 F.3d 629, 2004 U.S. App. LEXIS 15354 (6th Cir. Mich., 2004)

Walter, Volker. “Object-Based Classification of Remote Sensing Data for Change Detection.” *ISPRS Journal of Photogrammetry and Remote Sensing* 58 (2004): 225–38.

Whigham, D. F. 1999. *Ecological issues related to wetland preservation, restoration, creation and assessment.* The Science of the Total Environment 240(1999): 31 - 40.

Whitehead, Kenneth, and Chris Hugenholtz. “Remote Sensing of the Environment with Small Unmanned Aircraft Systems (UASs), Part 1: A Review of Progress and Challenges.” *Journal of Unmanned Vehicle Systems*, no. ja (2014).

Young, T. P. 1999. *Restoration ecology and conservation biology*. Biological Conservation 92 (2000): 73- 83.

Zaman, B., A.M., Jensen, and M. McKee. *Use of high-resolution multispectral imagery acquired with an autonomous unmanned aerial vehicle to quantify the spread of an invasive wetlands species.* Vancouver, BC: IEEE.

Zhang, Caiyun, and Zhixiao Xie. “Combining Object-Based Texture Measures with a Neural Network for Vegetation Mapping in the Everglades from Hyperspectral Imagery.” *Remote Sensing of Environment* 124 (2012): 310–320.